NASA Technical Memorandum 84613

Bending Stiffness of Multiwall Sandwich

Max L. Blosser

APRIL 1983

25th Anniversary
1958-1983

NASA

NASA Technical Memorandum 84613

Bending Stiffness of Multiwall Sandwich

Max L. Blosser
Langley Research Center
Hampton, Virginia

National Aeronautics
and Space Administration

**Scientific and Technical
Information Branch**

1983

SUMMARY

An analytical and experimental study was carried out to understand the extensional and flexural behavior of multiwall sandwich, a metallic insulation composed of alternate layers of flat and dimpled foil. The multiwall sandwich was structurally analyzed by using several simplifying assumptions combined with a finite element analysis. The simplifying assumptions made in this analysis were evaluated by bending and tensile tests. Test results validated the assumption that flat sheets in compression do not significantly contribute to the flexural stiffness of multiwall sandwich for the multiwall geometry tested. However, calculations showed that thicker flat sheets may contribute significantly to bending stiffness and cannot be ignored.

Both test data and results of a finite element analysis show that the dimpled sheet is stiffer in the 0° direction than in the 45° direction. Tensile tests show that in the 0° direction, the dimpled sheet behaves linearly until material yielding occurs; however, in the 45° direction the dimpled sheet exhibits nonlinear behavior as a result of significant shape changes. The nonlinear behavior is strongly dependent on the lateral-edge constraint of the dimpled sheet. Two sets of boundary conditions were used in the linear finite element analysis to bracket the actual constraint of the dimpled sheet in the multiwall sandwich. Results of this analytical approach compare well with test data; both show that the extensional stiffness of the dimpled sheet in the 0° direction is about 30 percent of that for a flat sheet, and that in the 45° direction, it is about 10 percent. The analytical and experimental multiwall bending stiffnesses showed good agreement for the particular geometry tested.

INTRODUCTION

Multiwall sandwich is a unique structural sandwich concept, which was originally designed as a vacuum-sealed insulation for cryogenic tankage (ref. 1). As an outgrowth from this concept, several studies have considered an unsealed version of the multiwall sandwich for use as a thermal protection system (TPS) (refs. 2 to 4). An exploded view and cross section of a typical TPS tile made of multiwall sandwich are shown in figure 1. The sandwich consists of alternate layers of flat and dimpled, foil-gauge metal sheets bonded together at the crests of the dimples. As shown in the cross-sectional view, bonding of the flat and dimpled sheets forms a complex, three-dimensional structure.

Although designed primarily from thermal considerations to be a lightweight insulation, the multiwall sandwich must also be designed to carry the loads to which it will be subjected in TPS applications. Structural analysis of multiwall is complicated by buckling of the flat sheets loaded in compression and by the complex shape of the dimpled sheet. In the initial conceptual development of multiwall for TPS application, reference 3, approximate engineering-type calculations were developed for preliminary structural analysis. These calculations are based on the assumptions that (1) flat sheets in compression were totally ineffective, (2) dimpled sheets were fully effective in both tension and compression, and (3) each dimpled sheet could be represented as a flat sheet located at the centroid of the dimpled sheet.

The purpose of this paper is to study the structural behavior of multiwall sandwich (referred to as multiwall) and to develop a more refined, but still approximate, method for calculating its flexural stiffness. Results from tensile tests of dimpled sheets and bending tests of multiwall-sandwich specimens are used to evaluate some of the analytical assumptions and to provide experimental data for comparison with analytical predictions.

SYMBOLS

A	effective area per unit width of each sheet, used to calculate moment of inertia (see appendix B), $in^2/in.$
a	distance from outer support to inner load application point in four-point bending tests (see appendix D), in.
b	arbitrary column width, used for buckling calculations (see appendix A), in.
d	distance from neutral bending axis, in.
E	material modulus of elasticity, psi
E_{eff}	effective modulus of elasticity, average stress divided by average strain, psi
h_d	dimple height, the vertical distance between dimple peaks and troughs (see appendix B), in.
I	bending moment of inertia per unit width, $in^4/in.$
L	length of the boundary on the finite element model, in.
ℓ	distance between inner load application points in four-point bending tests (see appendix D), in.
M	bending moment, in-lb
M_0	constant bending moment applied to center section of four-point bending specimens (see appendix D), in-lb
n	number of effective sheets in a multiwall sandwich under bending (see appendix B)
P	applied load in bending tests (see appendix D), lb
R	ratio of the thickness of a flat sheet to that of a dimpled sheet with the same extensional stiffness
s	distance between nodes along the 45° direction in dimpled sheets, in.
t_d	dimpled-sheet thickness before forming, in.
t_f	flat-sheet thickness, in.

t_{face} face-sheet thickness, in.

w transverse displacement of beam, in.

$\bar{y}$ distance from lower surface of sandwich to neutral bending axis (see appendix B), in.

δ measured displacement in bending tests, in.

σ stress, psi

Subscripts:

ab after flat sheets buckle

av average

bb before flat sheets buckle

cr critical

0° flat sheet supported by a dimpled sheet oriented in the 0° direction

45° flat sheet supported by a dimpled sheet oriented in the 45° direction

ANALYSIS

The assumptions used for the structural analysis of the multiwall sandwich are similar to those of reference 3. Since the structural behavior of flat sheets is well understood, the flat sheets were analyzed using standard techniques. Thus, the majority of the analytical effort in this paper is focused on the dimpled sheets because of their complex geometry. First, the extensional stiffnesses of the flat sheets in tension and compression are determined. The extensional stiffness of the dimpled sheet is separately determined. Then these extensional stiffnesses are used in simple beam theory calculations to estimate the bending stiffnesses of various configurations of multiwall sandwich.

Extensional Stiffness

Flat sheets.- Because their primary function is to provide radiation barriers, the flat sheets, which are supported on the crests of the dimpled sheets, are made thin to reduce weight. Although they were assumed to be fully effective in tension, the thin flat sheets will buckle in compression at low stress. Appendix A shows the calculated compressive buckling stress of a flat sheet as a function of thickness. Since the buckling stress is very low for thin flat sheets, and thin sheets are likely to be prewrinkled, the flat sheets were assumed (as in ref. 3) to buckle immediately in compression and to have no significant postbuckling stiffness.

Dimpled sheets.- In reference 3 the dimpled sheet was assumed to have the same inplane extensional stiffness as a flat sheet of the same thickness. To obtain a better estimate of the extensional stiffness, the dimpled sheet was analyzed using a finite element computer program, the SPAR structural analysis system (ref. 5). In this analysis the dimpled sheet was assumed to be linearly elastic and uniform in

thickness. The thickness used for the finite elements was obtained by multiplying the thickness of the dimpled sheet before forming t_d by the ratio of the surface area of the flat sheet to that of the dimpled sheet.

Two finite element models of the dimpled sheet were necessary because the geometries are different in the 0° orientation and the 45° orientation (see fig. 2). Since the dimpled sheet has a repeating geometric pattern, only the small regions indicated in figure 2 were modelled.

The finite element models, which represent the curved, three-dimensional surface of the dimpled sheet, are shown in figure 3. In both models, the tops of the dimples were assumed to be parallel to the midplane of the dimpled sheet. Boundaries 1 and 2 for the 0° direction model consist of two straight lines. One extends across the flat top of the dimple, and a second extends from the edge of the dimple top to the midplane. The diagonal connecting the intersection of boundaries 1 and 2 to the intersection of boundaries 3 and 4 consists of a straight line across the flat top of the dimpled sheet and a circular arc which is tangent to the midplane and connects to the edge of the dimple top. All four boundaries of the 45° model have the same shape as the diagonal of the 0° model. The diagonal connecting the dimples in the 45° model has a shape similar to boundaries 1 and 2 of the 0° model. The perpendicular diagonal is a straight line lying in the midplane. Triangular bending elements were used because the quadrilateral bending elements of SPAR require all four corner nodes to be coplanar for an accurate solution. To insure the symmetry of the structural response, the triangular elements were superimposed as shown in figure 4, and each element was assigned only half of the material modulus so that the model would have the correct stiffness. As shown in figure 4, there is no node in the finite element model at the intersection of the diagonals of the overlapping triangular elements. The model oriented in the 0° direction, shown on the left-hand side of figure 3, contains 100 nodes and 238 elements, and the model shown on the right-hand side of figure 3 and oriented in the 45° direction, contains 200 nodes and 656 elements.

For the model oriented in the 0° direction, boundaries 1 and 2 were treated as symmetry planes; i.e., translations and rotations about axes parallel to the plane of symmetry were constrained. Two different constraint cases were considered for boundary 3. In the first case, the boundary nodes were not allowed to translate in the x direction, and any lateral displacements were completely prevented. In the second case, a precalculated translation in the x direction was imposed on the boundary plane so that no net force existed normal to the boundary. The actual lateral constraint provided to the dimpled sheet by the flat sheets in multiwall has not been determined, but it is bounded by these two cases. Displacement of the nodes on boundary 3 in the z direction was not allowed in either case. The model was loaded by a uniform displacement applied in the y direction to each node on boundary 4.

For the model oriented in the 45° direction (fig. 3), the constraints applied to boundaries 1 and 2 were the same as those applied to boundaries 1 and 2 of the 0° models; that is, they were treated as symmetry planes. The same two constraint conditions were applied to the x displacement of boundary 3 as for the 0° model to provide upper and lower bounds to the actual lateral constraint on the dimpled sheet in the multiwall sandwich. The nodes on boundaries 3 and 4 were not constrained from translation in the z direction but were constrained from rotation about the y and x axes, respectively. Also nodes on boundaries 3 and 4 were constrained from rotation about the z axis. The node at the corner of boundaries 1 and 4, the node at the corner of boundaries 2 and 3, and the node midway between these two corners were fixed in the z direction.

The extensional stiffness of the dimpled sheet was determined from the applied displacements and the reaction forces calculated by using the SPAR finite element program. Average stress was calculated by dividing the sum of the reactions on the boundary opposite the applied displacement by the cross-sectional area $t_d L$ of the model. The average strain was determined by dividing the applied displacement by the length of the model in the direction of displacement. The average stress was divided by the average strain to get an effective modulus E_{eff}. The extensional stiffness per unit width of the dimpled sheet is then $E_{eff} t_d$. Since the extensional stiffness of a flat sheet per unit width is Et_f, the thickness of a flat sheet which will have the same extensional stiffness as the dimpled sheet is

$$t_f = Rt_d$$

where

$$R = \frac{t_f}{t_d} = \frac{E_{eff}}{E}$$

Thus R indicates the reduced extensional stiffness of a dimpled sheet.

In addition to stiffness, the stress distribution in a dimpled sheet under an extensional loading was also determined by finite element analysis. The finite element models for both the 0° and 45° directions were refined by adding additional nodal points and triangular bending elements in areas of high stress to create the models shown in figure 5. The loading and boundary conditions remained the same. Stresses were calculated in the x and y directions and on the upper, middle, and lower surfaces at each node of boundaries 1 and 2 (fig. 5). These stresses were then divided by the overall average stress to obtain the stress concentration factors.

Sandwich Bending Stiffness

Once the extensional behavior of the flat and dimpled sheets is known, the moment of inertia and hence the bending stiffness of the multiwall sandwich can be easily calculated using standard engineering techniques. If the individual flat and dimpled sheets are assumed to have negligible bending stiffness compared with the total sandwich, the bending moment will be carried entirely by axial forces in the flat and dimpled sheets. By using some of the assumptions from reference 3, which are illustrated in figure 6, the moment of inertia of a multiwall sandwich can be determined by simple beam theory calculations. The sketch on the left of figure 6 represents the actual multiwall sandwich loaded in bending. The right-hand sketch illustrates the idealized structure in which flat sheets in compression have been removed entirely to simulate their buckling. Dimpled sheets have been replaced by flat sheets with their thicknesses reduced to represent the associated reduced extensional stiffness, and flat sheets in tension remain unchanged. Because the flat sheets in compression buckle and carry little load, the neutral bending axis is no longer at the geometric center of the structure. Calculations of moment of inertia for sandwiches of one, two, and three dimpled layers are shown in appendix B. Moment of inertia is used as a measure of bending stiffness because, for linear behavior, it is independent of material.

TESTS

Tensile and bending tests were required to verify the assumption that thin, flat sheets in compression can be ignored and to determine experimentally the extensional stiffness of the dimpled sheet and the bending stiffness of various multiwall sandwich configurations for comparison with analysis. The stiffness properties of interest, R for the dimpled sheet and I, moment of inertia, for the multiwall sandwich, are dependent only on geometry and should be independent of material. Therefore, any linearly elastic material can be used. Most of the tensile specimens and all the bending specimens were made of stainless steel because it was more readily available and more easily formed. However, since the present multiwall TPS tiles are made of titanium, some titanium tensile specimens were also tested.

Sheet Tensile Tests

Specimen fabrication. - Dimpled sheet specimens were fabricated from type 304 stainless steel and 6Al-4V titanium, which were 0.004 and 0.003 in. thick, respectively. The dimpled sheets were formed from 12-in. by 24-in. flat sheets by using dies having evenly spaced but offset grids of protruding pins. The stainless steel sheets were cold formed; however, the titanium sheets were superplastically formed at an elevated temperature. Dogbone-shaped, stainless steel specimens, 10 in. long and 1.5 in. wide at the test section, and 3-in. by 12-in. rectangular titanium specimens were cut from the dimpled sheets in both 0° and 45° orientations with an electronic discharge machine (EDM).

Test setup and procedure. - The specimens were loaded in a universal test machine, with the machine crosshead moving at a constant rate of 0.1 in/min. Load was measured by a simple reading from a load cell in the machine; however, difficulties were encountered in attempting to measure strain. Standard strain gauges could not be used to measure average strain because of the uneven surface of the specimens. This uneven surface also made it difficult to properly attach available extensiometers to the specimen. Because the specimens were tested at low loads and the test machine was designed for much higher loads, the strain was assumed to be the displacement of the machine crosshead divided by the original length of the specimen between the grips. Thus, input from the load cell and from the motion of the crosshead were used to record load-deflection curves on the chart recorder of the test machine.

Sandwich Bending Tests

Specimen fabrication.- Bending test specimens, shown in figure 7, were fabricated from 12-in. by 24-in. sheets of type 304 stainless steel brazed together. The flat sheets were 0.002 in. thick, and the dimpled sheets were 0.004 in. thick before dimpling. The dimpled and flat sheets were assembled to make multiwall panels of one, two, and three dimpled layers. Holes were drilled, and pins were inserted through the corners of the panels to assure alignment of the dimpled sheets. The assembled dimpled and flat sheets were brazed at 1470°F for 2 to 4 min in a vacuum furnace. For each of the one-, two-, and three-layer configurations, specimens (2 in. by 11 in.) were fabricated with dimpled sheets oriented in the 0° direction and in the 45° direction.

Test setup and procedure. - A sketch of a standard four-point bending test arrangement is shown in figure 8. The specimen was supported by 1/2-in-diameter

steel rods spaced 10 in. apart in a metal framework, which rested on top of a load cell. The load was applied through two 1/2-in-diameter steel rods, spaced 6 in. apart and attached to the moving machine head of a universal test machine. The deflection was measured from the center of the specimen relative to the moving machine head by using a direct current displacement transducer (DCDT). Load-deflection curves were recorded by a flat-bed plotter from the output of the DCDT and the load cell.

Multiwall specimens of one, two, and three dimpled layers with dimpled sheets oriented in both the 0° and 45° directions were tested in four-point bending tests. Each specimen was loaded to a point in the linear range of the load-deflection curve and unloaded two times prior to loading to failure. Thus, at least three load-deflection curves were recorded for each specimen. The specimens were first tested intact to obtain their experimental bending stiffnesses. Then, for each of the one- and two-dimpled-layer specimens, the outer flat sheet which had been in compression was cut at each dimple pitch so that it could carry no load. These specimens were retested to determine how much the flat sheets in compression contributed to flexural stiffness of the multiwall sandwich. Then the other outer flat sheet of each two-dimpled-layer specimen was also cut so that only the two dimpled layers remained to carry the bending load. These two-dimpled-layer specimens were retested, and the data were used to determine the extensional stiffness of the dimpled sheet by the method in appendix C.

RESULTS

Extensional Stiffness

Flat sheets. - One of the key assumptions in the multiwall design approach presented herein and in reference 3 is that flat sheets in compression buckle at a low load and have a negligible contribution to flexural stiffness. Results of bending tests on one- and two-dimpled-layer specimens indicate this assumption is valid when the flat sheets are 0.002 in. thick. Figure 9 shows how the flat sheets in compression affect the moment of inertia of multiwall bending specimens. The moment of inertia, which is proportional to bending stiffness, is shown for four different multiwall configurations. The method used to calculate the experimentally determined moments of inertia from the load-deflection curves is presented in appendix D. The unshaded bars in figure 9 represent the moment of inertia of intact specimens, and the shaded bars represent the moment of inertia of specimens with the flat sheets in compression effectively removed. The moments of inertia are nearly the same for the intact specimens and the cut specimens. Thus, it appears to be a valid assumption to ignore the 0.002-in-thick flat sheets in compression when calculating bending stiffness of multiwall.

If, however, these flat sheets are thicker than 0.002 in., they may have a significant contribution to the bending stiffness. The calculations described in appendix E and summarized in figure 10 indicate the effect that thicker flat sheets would have on the behavior of a multiwall sandwich in bending. Figure 10 shows the predicted deflection curves which would be obtained in four-point bending tests of two-dimpled-layer specimens with flat sheets of different thickness. These curves were calculated by assuming that the flat sheets buckle at stresses predicted in appendix A and that the flat sheets have no post buckling stiffness. The initial slope of each curve reflects the flexural stiffness before the flat sheets buckle, and the final slope reflects the bending stiffness after the flat sheets buckle. The horizontal portion of each curve represents the load at which the flat sheets reach

their compressive buckling stress. The dashed line is a load-deflection curve measured for a specimen with 0.002-in. flat sheets. The slope of the measured curve is close to that predicted for the specimen with buckled flat sheets at low loads. These calculations indicate that the flexural behavior of the multiwall sandwich is sensitive to the flat-sheet thickness and that the assumption that flat sheets buckle and carry no further load in compression is not valid as flat-sheet thickness is increased.

A comparison of the approach taken in this paper with that of reference 6 illustrates the importance of the flat-sheet behavior in compression. The multiwall bending specimens tested in reference 6 had 0.003-in-thick flat sheets. The flat sheets remained unbuckled for a measurable portion of the load-deflection curve, and bending stiffnesses in reference 6 are calculated from the initial slope of the load-deflection curve, where the flat sheets were not buckled. As a result, the stiffnesses presented in reference 6 are much higher than would be predicted by the analysis presented in this paper.

Dimpled sheets. - Another key assumption in the multiwall design approach is that the structure exhibits linear behavior. Since high stresses can cause material nonlinearity, stress concentration factors were calculated for the dimpled sheet. Figure 11(a) shows stress distributions for the 0° orientation of the dimpled sheet calculated with the SPAR structural analysis system. Stresses are normalized by the average stress in the direction of loading, so that the curves shown represent stress concentration factors. Stress concentrations are shown on the boundaries, which are the locations of maximum stress on the model. Curves are shown for the upper, center, and lower surfaces of the bending elements. The large differences between stresses on the upper and lower surfaces indicate bending. The locations and signs of the bending stresses correspond to observed deformation of tensile test specimens. The large bending stresses along the x axis correspond to the observed flattening of the dimple. Along the $x = L$ boundary, the stress concentrations indicate there is little bending. However, the maximum principal stresses, which are within 10° of the y-direction stresses, indicate that much of the load is being carried along this path. The stress concentrations are high along both boundaries and exceed 4 at several locations.

Similarly, stress concentrations were calculated for both constraint cases of the dimpled sheet oriented in the 45° direction. Figure 11(b) shows the stress concentrations for the case of an allowed lateral displacement. This constraint case approximates the behavior of the dimpled sheet tensile test. As in figure 11(a), curves are shown for the upper, center, and lower surfaces of the bending elements. These curves indicate that there are very large stress concentrations due to bending along both boundaries of the model. The stress concentrations due to bending exceed 25 at the lower right-hand corner of the model. The reason for these large stress concentrations is apparent. The dimpled sheet tends to stretch in the direction of loading and to narrow or contract transverse to the direction of loading. Both of these deformations are resisted primarily by localized bending, which results in large bending stresses.

Stress concentrations for the case of no lateral displacement of the 45° dimpled sheet are shown in figure 11(c). Although the stress concentrations have a distribution similar to that in the previous example, the magnitudes of the stress concentrations are less than one quarter those of the 45° dimpled sheet with lateral displacement. The maximum stress concentration factor is about 6 and, again, is located in

the lower right-hand corner of the model. This dramatic decrease in bending stress illustrates how the structural behavior of the dimpled sheet is strongly dependent on the lateral constraint.

Stress-strain curves measured from tensile tests of both stainless steel and titanium dimpled sheets are shown in figure 12. The stress shown is the average stress obtained by dividing the load by the cross-sectional area. The average strain was determined by dividing the machine-head motion by the original length of the specimen. For a flat sheet tested in the same machine over the same load range as the dimpled sheet, the strain was measured by a strain gauge and found to be approximately half that determined from machine-head motion. Therefore, the strain should be approximately half of that shown in figure 12. Although the strain is not accurate, the curves in figure 12 illustrate the characteristic behavior of the dimpled sheets and the differences in behavior between sheets oriented in the 0° and 45° directions.

Both the stainless steel and titanium dimpled-sheet specimens show similar behavior in the 0° direction. The specimens behave linearly until the material yields and the stiffness is reduced. The dimples tended to flatten, and there was no noticeable narrowing of the specimen. The predicted average stresses at which local material yielding occurs for the 0° dimpled sheet are indicated on figure 12. This stress was calculated by dividing the material yield stress (stainless steel, 42 000 psi; titanium, 130 000 psi) by the largest stress concentration factor (4.9) from figure 11(a). These predicted stresses are close to the stresses where the dimpled sheets begin to show nonlinear behavior. The stress-strain curve for the 0° direction indicates that the linear finite element analysis will be adequate to predict the behavior of the 0° dimpled sheet at low loads.

The dimpled sheet exhibits completely different behavior in the 45° direction. The stress-strain curves of the 45° dimpled sheet (see fig. 12) show that at low loads, the dimpled sheet has little stiffness, but as the load increases, the stiffness also increases. This increased stiffness is caused by the specimen changing shape under load. Figure 13 shows a stainless steel, 45° dimpled-sheet specimen before and after deformation under a tensile load. Each vertical line of dimples is pulled into a corrugation, and the specimen is narrowed significantly, as indicated by the dashed lines. Although the dimpled-sheet specimen is obviously deformed considerably beyond the range of linear behavior, the figure illustrates the type of deformation which occurs.

To understand this observed nonlinear behavior, it is helpful to consider a dimpled sheet loaded in tension as a series of parallel beams loaded in tension. In the 0° direction, some of these beams are straight and provide a straight-through load path, while others are wavy. The straight beams act as rods and carry the load in tension, but the wavy beams carry the load primarily through bending. The straight beams are therefore much stiffer and, consequently, carry more of the load. As the load increases, the strain increases, and the curved beams begin to straighten out, which results in flattening of the dimples.

For the 45° direction, it is helpful to consider the dimpled sheet as a lattice of straight and wavy beams crisscrossed at ±45°. There is no straight-through load path. That is why the dimpled sheet has less stiffness in the 45° direction than in the 0° direction. When this lattice is loaded in tension, the straight beams tend to rotate to align themselves with the load. This induces lateral contraction, which causes the dimpled sheet to narrow significantly and to fold into corrugations with

crests running parallel to the direction of the applied load. The resulting corrugated shape significantly reduces the curvature of the wavy beams and correspondingly increases the overall stiffness of the dimpled sheet.

The importance of lateral boundary constraint becomes apparent when considering the 45° dimpled sheet as a lattice of rods. When the lateral edge is unconstrained, as in the tensile test, the lateral contraction is resisted only by localized bending of the dimpled sheet; however, when the edge is constrained, the lateral contraction is resisted at the boundary, and the localized bending is inhibited. Since this shape change is reduced, the behavior of the dimpled sheet should be more nearly linear. In the multiwall sandwich, a partial lateral constraint is imposed on the dimpled sheet by the flat sheets and other dimpled sheets. Consequently, the 45° dimpled sheet may show more nearly linear behavior in the multiwall sandwich than in the tensile tests.

Although the stress-strain curves of both the stainless steel and titanium 45° dimpled sheets (see fig. 12) show the same trends, their shapes are somewhat different. The two most likely causes are different thicknesses and different materials. The stainless steel dimpled sheet was 0.004 in. thick and the titanium sheet was 0.003 in. thick; however, analysis indicates that this difference in thickness would not cause the behavior to differ as much as observed. Stainless steel has a yield point which is one-third that of titanium. Considering the high initial stress concentration factors predicted by the finite element analysis, some localized yielding is likely to occur in the stainless steel before it would occur in the titanium. This localized yielding may enable the stainless steel to deform more quickly into the stiffer shape. The offsetting factors of increased stiffness due to shape change and decreased stiffness due to localized yielding may result in the shape of the stainless steel stress-strain curve.

Because the tensile test specimens did not have lateral boundary conditions representative of the multiwall sandwich, bending tests of sandwich specimens were used to measure the extensional stiffness of the dimpled sheet. The method used to calculate the extensional stiffness of the dimpled sheet from the measured load-deflection curves is presented in appendix C. In figure 14 the dimpled sheet extensional stiffnesses obtained from bending tests are compared with those predicted using the SPAR finite element program. The extensional stiffness is indicated in terms of R, which is the ratio of the thickness of a flat sheet t_f to that of a dimpled sheet t_d with the same extensional stiffness. Therefore, by definition, for a flat sheet, $R = 1$. The open circles represent the extensional stiffness of the 0° dimpled sheet, and the triangles represent that of the 45° dimpled sheet obtained from bending tests. Each symbol represents a single specimen. The curves on the left-hand side of the figure represent the extensional stiffnesses of the dimpled sheet calculated for various dimpled-sheet thicknesses t_d and a constant dimple height h_d. The curves on the right-hand side represent extensional stiffnesses calculated for various dimple heights h_d and a constant dimpled-sheet thickness t_d. The upper narrow band represents the calculated extensional stiffness for the 0° direction; the lower wide band represents the calculated extensional stiffness for the 45° direction. The experimental and predicted results agree well in that they both show the extensional stiffness of dimpled sheet in the 0° direction to be about 30 percent that of a flat sheet, and in the 45° direction to be about 10 percent that of a flat sheet. For the 0° direction the predicted stiffness falls within the experimental scatter, and for the 45° direction the test data fall within the predicted range.

Bending Stiffness

In figure 15 moments of inertia determined from the bending tests of multiwall specimens with one, two, and three dimpled layers are compared with moments of inertia predicted using values of R calculated by the finite element analysis. The shaded bars represent experimental values, and the unshaded bars represent analytical values. The experimental values were obtained from the measured load-deflection curves by the method given in appendix D, and the predicted values were obtained by the method given in appendix B. Since a range of R was predicted by the finite element analysis because of lateral displacement boundary conditions, there is a corresponding range of calculated values of moment of inertia indicated by the arrows. The experimental values fall well within this range. Considering the complex behavior of the dimpled sheet observed during tensile tests, the agreement between analysis and experiment is surprisingly good. Although the dimpled sheet behaves nonlinearly in tension, multiwall sandwich specimens with dimpled sheets oriented in the 0° or 45° direction exhibited linear behavior in bending. These results indicate that the bending stiffness of the multiwall sandwich can be determined by a relatively simple engineering approach. However, additional test data are required to confirm this conclusion for other multiwall geometries and fabrication methods.

CONCLUDING REMARKS

An analytical and experimental study was carried out to understand the structural behavior of multiwall sandwich. The two primary components of multiwall sandwich, flat sheets and dimpled sheets, were analyzed separately to determine behavior in tension and compression. Once this behavior was known, the moment of inertia of the multiwall sandwich, which is proportional to bending stiffness, was determined using standard engineering calculations. Test data were obtained to evaluate the accuracy of these bending stiffness calculations and to evaluate the assumptions used in the analysis.

Comparison of the test data with the calculated values verifies the assumption that the flat sheets which are loaded in compression during bending will buckle, carry little load, and can be ignored. However, the flat sheets in these specimens were only 0.002 in. thick, and calculations indicate that thicker flat sheets will carry a more significant load before buckling. Consequently, the assumption that flat sheets in compression can be ignored becomes less valid if the thickness of the sheets is increased.

Both the finite element analysis and the test data show that the dimpled sheet has significantly less stiffness than a flat sheet of the same thickness. Also, analysis and experiment show that the dimpled sheet has directional properties and is significantly stiffer in the 0° direction than in the 45° direction. Tensile tests show that in the 0° direction, the dimpled sheet behaves linearly until material yielding occurs; however, in the 45° direction, the dimpled sheet exhibits nonlinear behavior as a result of its significant shape changes. Finite element analysis shows that high local bending stresses occur in the tensile specimens and that the associated shape changes are strongly influenced by the lateral-edge constraints. The dimpled sheets in the multiwall sandwich are not free from lateral-edge constraint. Therefore, the behavior of the 45° dimpled sheet in the multiwall sandwich may be much more nearly linear than that observed in the tensile tests. Two constraint cases were used in the analysis to bracket the actual lateral constraint

imposed on the dimpled sheet in the multiwall sandwich. Results of this analytical approach compare well with test data. Both show that the extensional stiffness of the dimpled sheet in the 0° direction is about 30 percent of that for a flat sheet, and that in the 45° direction, it is about 10 percent.

The predicted multiwall-sandwich bending stiffness agrees surprisingly well with experiment for all sandwich configurations tested. Although the dimpled sheet behaves nonlinearly in tension, multiwall-sandwich specimens with dimpled sheets oriented in the 0° or 45° direction exhibited linear behavior in bending. The close agreement between analysis and experiment indicates that the method of calculating bending stiffness presented in this paper is valid for this linear range of behavior. However, for other multiwall geometries and fabrication methods, this method may be less accurate.

Langley Research Center
National Aeronautics and Space Administration
Hampton, VA 23665
March 11, 1983

APPENDIX A

BUCKLING OF FLAT SHEETS IN COMPRESSION

The flat sheets which are in compression during bending are assumed to buckle at a low stress and, consequently, to carry no load. The calculations in this appendix estimate the buckling stress of the flat sheet. Since only uniaxial bending is considered, buckling of the flat sheets is approximated using column theory. The buckling load should be lower than predicted because the boundary condition is actually between simply supported and clamped, and the foil-gauge sheet will likely not be perfectly flat.

The following sketch represents a flat sheet in uniaxial compression. Each dot represents a point at which the flat sheet is supported by a dimpled sheet oriented in the 0° direction. The curved lines represent alternate crests and troughs, which are the buckling shapes observed during the bending tests. The area enclosed by dashed lines was modelled as a clamped column, buckling in the second mode.

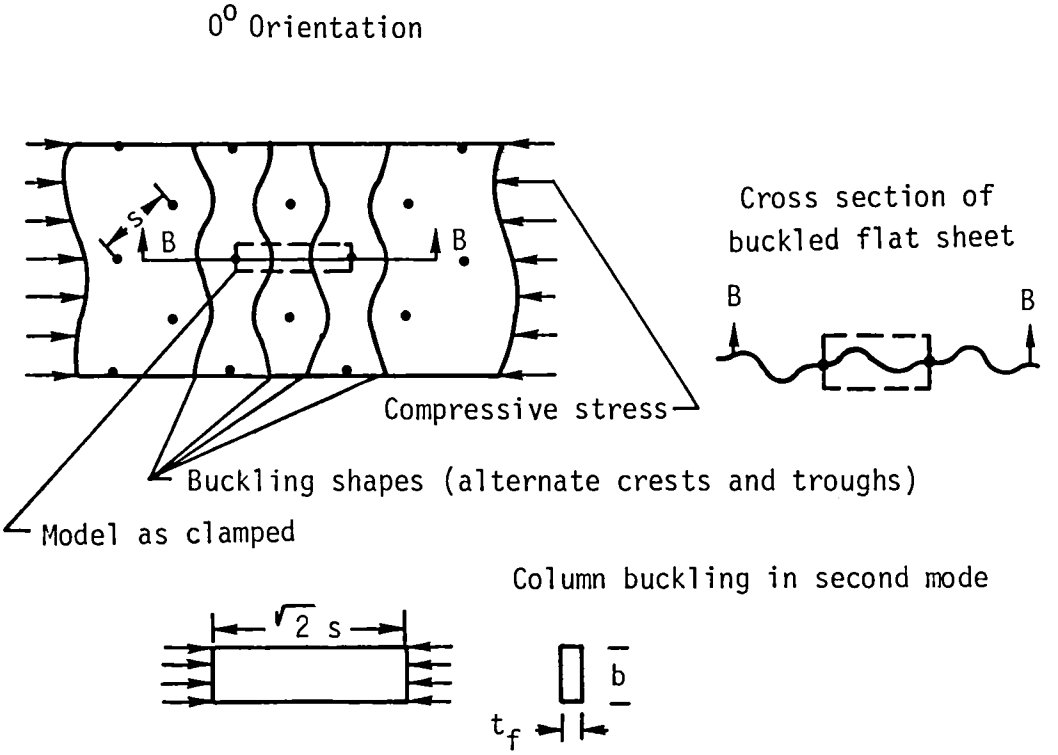

From column buckling theory,

$$(P_{cr})_{0°} = \frac{8.18\pi^2 EI}{(\sqrt{2}s)^2} \qquad \text{(A1)}$$

where $(P_{cr})_{0°} = (\sigma_{cr})_{0°} bt_f$, and $I = \frac{bt_f^3}{12}$.

By substitution,

$$(\sigma_{cr})_{0^\circ} = \frac{8.18\pi^2 E t_f^2}{24 s^2} \tag{A2}$$

A similar sketch is shown below for a flat sheet supported by a dimpled sheet oriented in the 45° direction. In this case, the observed buckling shape was much simpler. The flat sheet buckles upward between each lateral row of dimple peaks. Consequently, the area enclosed by the dashed lines was treated as a clamped column buckling in the first mode.

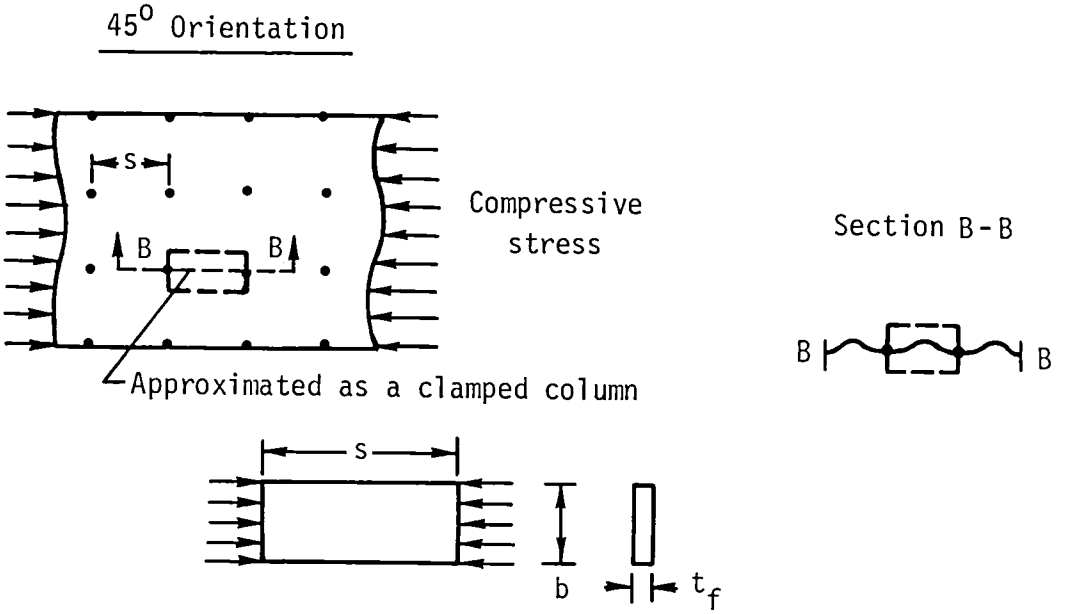

From column buckling theory,

$$(P_{cr})_{45^\circ} = \frac{4\pi^2 EI}{s^2} \tag{A3}$$

where $(P_{cr})_{45^\circ} = (\sigma_{cr})_{45^\circ} b t_f$, and $I = \frac{b t_f^3}{12}$.

By substitution,

$$(\sigma_{cr})_{45^\circ} = \frac{\pi^2 E t_f^2}{3 s^2} \tag{A4}$$

APPENDIX A

The following figure was generated from the two expressions for σ_{cr} developed in this appendix. The figure shows that the buckling stress is very low for the 0.002-in. flat sheets which were tested, but that the buckling stress increases quadratically as flat-sheet thickness increases.

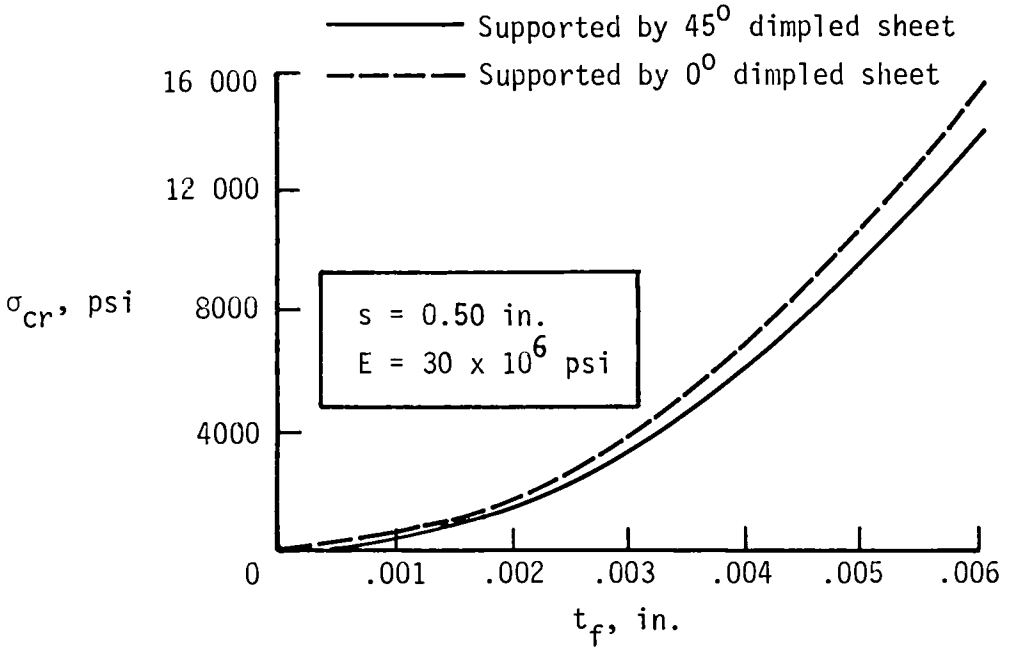

APPENDIX B

CALCULATION OF MOMENT OF INERTIA OF MULTIWALL BENDING SPECIMENS

This appendix contains calculations which predict the moment of inertia of the bending test specimens of one, two, and three dimpled layers. The flat sheets loaded in compression are assumed to buckle and carry no load. The dimpled sheet is modelled as a flat sheet with a reduced thickness lying along the midplane of the dimpled sheet. The reduced thickness represents the reduced stiffness associated with the dimpled sheet. The moment of inertia of the resulting model is then calculated using the parallel axis theorem.

One-Dimpled-Layer Multiwall Sandwich

The idealization of a one-dimpled-layer multiwall sandwich loaded in bending is shown in the following sketch.

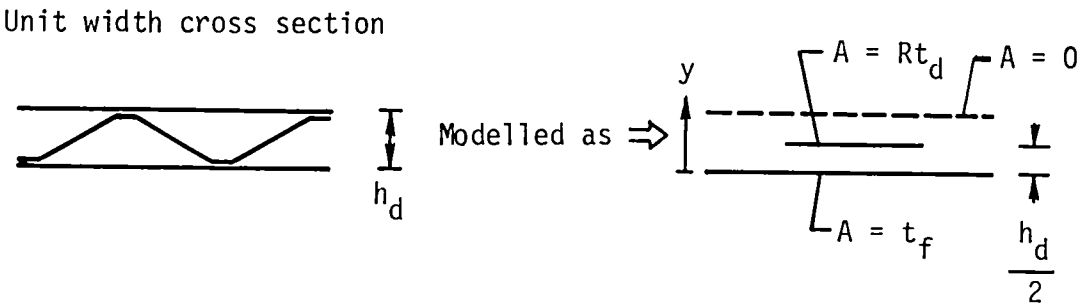

The neutral bending axis $\bar{y}$ is calculated by the following equation:

$$\bar{y} = \frac{\Sigma\, EAy}{\Sigma\, EA} \tag{B1}$$

For the one-dimpled-layer multiwall,

$$\bar{y} = \frac{(0)t_f + Rt_d\left(\frac{h_d}{2}\right)}{t_f + Rt_d} \tag{B2}$$

Once $\bar{y}$ is known, the moment of inertia I can be calculated from

$$I = \sum_{i=1}^{n} (I_i + d_i{}^2 A_i) \tag{B3}$$

where n is the number of sheets, and d is the distance from the neutral bending axis. The moment of inertia of each flat or dimpled sheet I_i is assumed to be negligible compared with the moment of inertia of the total sandwich.

$$I_i << I$$

Thus,

$$I = t_f(\bar{y})^2 + Rt_d\left(\frac{h_d}{2} - \bar{y}\right)^2 \tag{B4}$$

Two-Dimpled-Layer Multiwall Sandwich

The calculations are similar for a two-dimpled-layer sandwich. The following sketch shows the idealized structure.

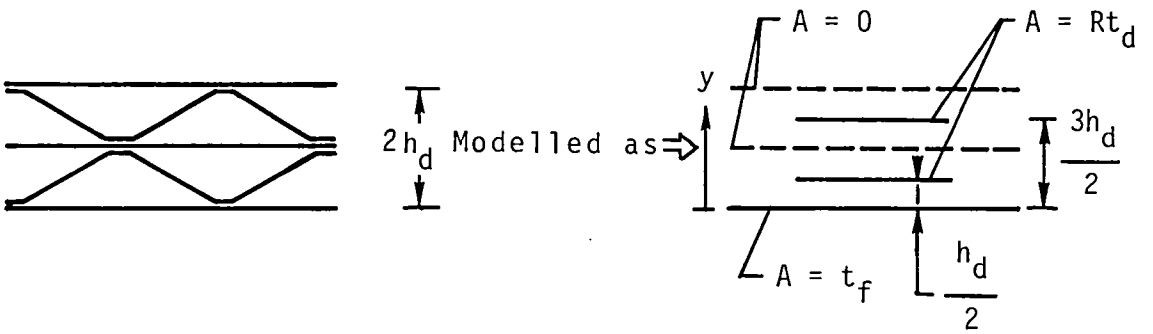

Again, the location of the neutral bending axis is calculated from equation (B1).

$$\bar{y} = \frac{(0)t_f + Rt_d\left(\frac{h_d}{2} + \frac{3h_d}{2}\right)}{t_f + 2Rt_d} \tag{B5}$$

where R is from figure 14. From equation (B3), the moment of inertia I is

$$I = t_f(\bar{y})^2 + Rt_d\left[\left(\frac{h_d}{2} - \bar{y}\right)^2 + \left(\frac{3h_d}{2} - \bar{y}\right)^2\right] \tag{B6}$$

APPENDIX B

Three-Dimpled-Layer Multiwall Sandwich

Similarily, for a three-dimpled-layer multiwall sandwich, the idealized structure is shown in the following sketch.

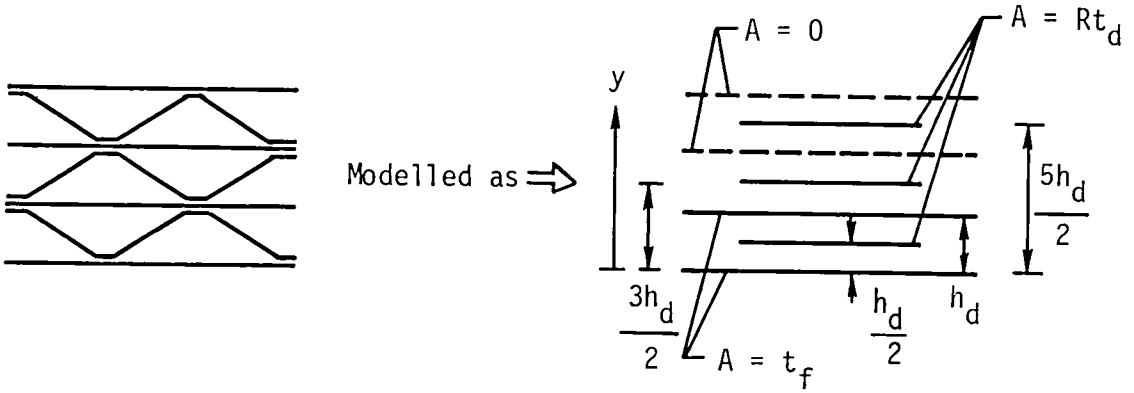

The neutral bending axis is

$$\bar{y} = \frac{t_f(0 + h_d) + Rt_d\left(\frac{h_d}{2} + \frac{3h_d}{2} + \frac{5h_d}{2}\right)}{2t_f + 3Rt_d}$$

Simplifying yields

$$\bar{y} = \frac{h_d\left(t_f + \frac{9}{2}Rt_d\right)}{2t_f + 3Rt_d} \tag{B7}$$

If $\bar{y} < h_d$, then the second-from-bottom flat sheet is loaded in compression and, thus, is effectively removed, and $\bar{y}$ must be recalculated.

If $\bar{y} < h_d$, then

$$\bar{y}^* = \frac{t_f(0) + \frac{9}{2}Rt_d h_d}{t_f + 3Rt_d} \tag{B8}$$

and

$$I = t_f(\bar{y}^*)^2 + Rt_d\left[\left(\frac{h_d}{2} - \bar{y}^*\right)^2 + \left(\frac{3h_d}{2} - \bar{y}^*\right)^2 + \left(\frac{5h_d}{2} - \bar{y}^*\right)^2\right] \quad \text{(B9)}$$

where $\bar{y}^*$ is the neutral bending axis calculated by assuming that all flat sheets except the bottom sheet have buckled.

If $\bar{y} > h_d$,

$$I = t_f[(\bar{y})^2 + (h_d - \bar{y})^2] + Rt_d\left[\left(\frac{h_d}{2} - \bar{y}\right)^2 + \left(\frac{3h_d}{2} - \bar{y}\right)^2 + \left(\frac{5h_d}{2} - \bar{y}\right)^2\right] \quad \text{(B10)}$$

APPENDIX C

CALCULATION OF R FROM EXPERIMENTAL DATA

This appendix contains the method of calculating R, the ratio of the stiffness of a dimpled sheet to that of a flat sheet with the same thickness, for a dimpled sheet using data from a four-point bending test. The moment of inertia of the two-dimpled-layer specimen, with upper and lower flat sheets cut to totally remove their contribution, was calculated from the load-deflection curve by the method given in appendix D. If the geometry of the dimpled sheet (sketch below) and the moment of inertia of the specimen are known, R for the dimpled sheet can be calculated in the following manner.

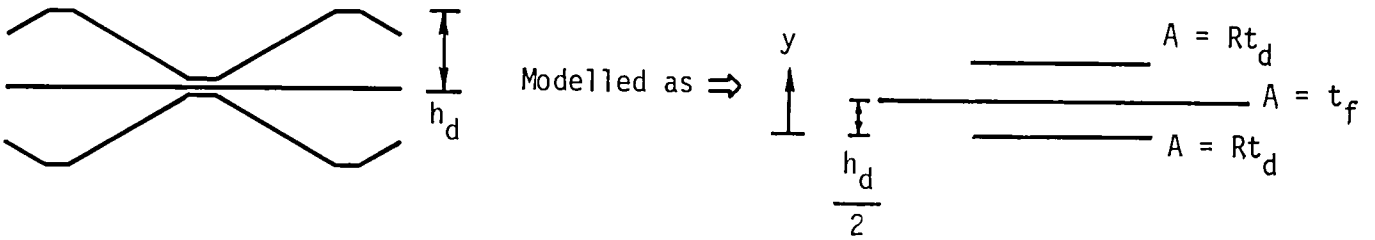

The neutral bending axis $\bar{y}$ is

$$\bar{y} = \frac{h_d}{2}$$

The moment of inertia I is

$$I = 2Rt_d\left(\frac{h_d}{2}\right)^2 \qquad \text{(C1)}$$

Thus,

$$R = \frac{2I}{t_d h_d^{\,2}} \qquad \text{(C2)}$$

(Use the experimentally determined value of I to obtain R.)

APPENDIX D

CALCULATION OF MOMENT OF INERTIA FROM FOUR-POINT BENDING TESTS

This appendix contains the method used to calculate the experimental moment of inertia from the measured loads and deflections of the test specimen. Deflections were measured at the center of the specimen, with respect to the points where the load was applied. The inner section of the specimen, between the points where the load was applied, was analyzed as a separate beam loaded in pure bending. An equation was developed relating the measured slope of the load-deflection curve to the moment of inertia of the specimen.

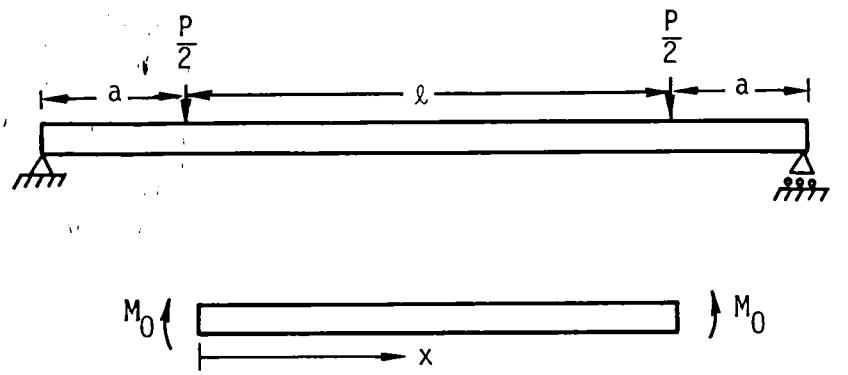

The central section of the specimen shown above can be treated as a separate beam of length ℓ loaded by pure bending $\left(M_0 = \frac{aP}{2}\right)$.

The moment-curvature relation for a beam is

$$EI \frac{d^2w}{dx^2} = M = M_0 = \frac{aP}{2} \qquad \text{(D1)}$$

where w = Transverse displacement. Integration gives

$$EI \frac{dw}{dx} = \frac{aP}{2} x + C_1$$

Applying the boundary condition to solve for C_1 yields

$$\frac{dw}{dx}\left(\frac{\ell}{2}\right) = 0 = \frac{aP\ell}{4} + C_1$$

$$C_1 = -\frac{aP\ell}{4}$$

Integrating again gives

$$EIw = \frac{aPx^2}{4} - \frac{aP\ell}{4}x + C_2$$

Applying the boundary condition to solve for C_2 yields

$$w_0 = 0 = C_2$$

$$w = \frac{aPx^2}{4EI} - \frac{aP\ell x}{4EI} \tag{D2}$$

At $x = \ell/2$, δ is the measured deflection.

$$w\left(\frac{\ell}{2}\right) = -\delta = \frac{aP\ell^2}{16EI} - \frac{aP\ell^2}{8EI}$$

$$\delta = \frac{aP\ell^2}{16EI} \tag{D3}$$

Solving for I gives

$$I = \frac{a\ell^2}{16E}\frac{P}{\delta} \tag{D4}$$

where P/δ is the measured slope of the load-deflection curve.

APPENDIX E

EFFECT OF FLAT-SHEET THICKNESS ON PREDICTED LOAD-DEFLECTION CURVES FOR FOUR-POINT BENDING TESTS

The calculations in this appendix show how the use of thicker flat sheets may affect the flexural behavior of multiwall sandwich. As an example, load-deflection curves were predicted for a four-point bending test of a two-dimpled-layer multiwall sandwich with dimpled sheets oriented in the 0° direction. The shape of the curve was predicted by calculating the slope of the curve before the flat sheet buckled, the load at which buckling occurred, and the slope after the flat sheet buckled.

To calculate the slope before buckling, the moment of inertia must be calculated. The following sketch shows an idealized two-dimpled-layer sandwich loaded in bending with no flat sheets buckled.

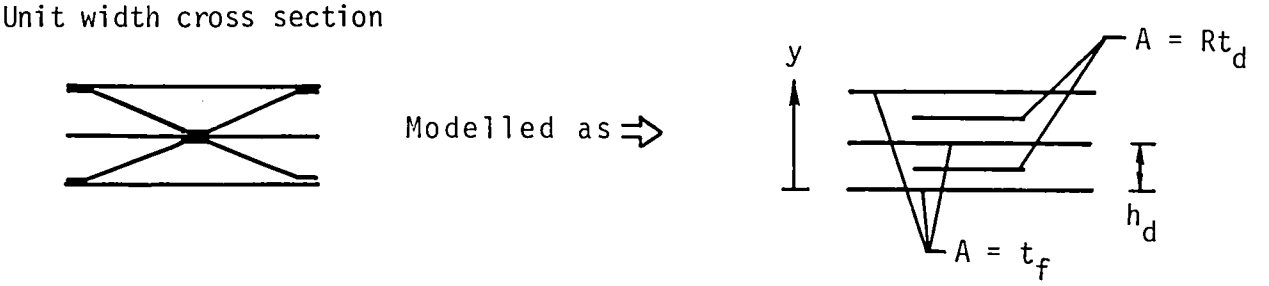

From equation (B3),

$$I_{bb} = \sum_{i=1}^{n} (I_i + d_i^2 A_i)$$

where n = Number of sheets and I_{bb} = I before buckling of flat sheets. Assuming $I_i \ll I$,

$$I_{bb} = h_d^2 \left(\frac{Rt_d}{2} + 2t_f \right) \tag{E1}$$

To obtain the slope before buckling, equation (D4) is used.

$$I_{bb} = \frac{a\ell^2}{16E} \frac{P}{\delta}$$

Thus, the slope of the load-deflection curve before flat sheets buckle is given by

$$\left(\frac{P}{\delta}\right)_{bb} = \frac{16EI_{bb}}{a\ell^2} \tag{E2}$$

To obtain the load at which buckling occurs, equation (A2) for buckling stress is used. For a flat sheet supported by a 0° dimpled sheet,

$$(\sigma_{cr})_{0°} = \frac{8.18\pi^2 E t_f^2}{24s^2}$$

And from simple beam theory,

$$\sigma = \frac{M(\bar{y} - y)}{I_{bb}} = -\frac{\frac{aP}{2} h_d}{I_{bb}} \tag{E3}$$

For $\sigma = (\sigma_{cr})_{0°}$,

$$\left|(P_{cr})_{0°}\right| = \frac{2I_{bb}(\sigma_{cr})_{0°}}{ah_d} = \text{Load at which flat sheet buckles} \tag{E4}$$

To determine the slope of the curve after buckling, the moment of inertia must be calculated from equation (B5).

$$\bar{y} = \frac{2Rt_d h_d}{t_f + 2Rt_d}$$

From equation (B6),

$$I \text{ after buckling} = I_{ab} = t_f(\bar{y})^2 + Rt_d\left[\left(\frac{h_d}{2} - \bar{y}\right)^2 + \left(\frac{3h_d}{2} - \bar{y}\right)^2\right]$$

From equation (D4),

$$\left(\frac{P}{\delta}\right)_{ab} = \frac{16EI_{ab}}{a\ell^2} = \text{Slope of curve after buckling of flat sheets} \tag{E5}$$

These equations were used to generate the curves shown in figure 10.

REFERENCES

1. Jackson, L. Robert; Davis, John G., Jr.; and Wichorek, Gregory R.: Structural Concepts for Hydrogen-Fueled Hypersonic Airplanes. NASA TN D-3162, 1966.

2. Jackson, L. Robert: Multiwall TPS. Recent Advances in Structures for Hypersonic Flight, NASA CP-2065, Part II, 1978, pp. 671-706.

3. Jackson, L. Robert; and Dixon, Sidney C.: A Design Assessment of Multiwall, Metallic Stand-Off, and RSI Reusable Thermal Protection Systems Including Space Shuttle Application. NASA TM-81780, 1980.

4. Shideler, John L.; Kelly, H. Neale; Avery, Don E.; Blosser, Max L.; and Adelman, Howard M.: Multiwall TPS - An Emerging Concept. NASA TM-83133, 1981.

5. Whetstone, W. D.: SPAR Structural Analysis System Reference Manual - System Level 13A. Volume I: Program Execution. NASA CR-158970-1, 1978.

6. Meaney, J. E.: Extensional, Bending and Twisting Stiffness of Titanium Multi-wall Thermal Protection System (TPS). NASA CR-165866, 1982.

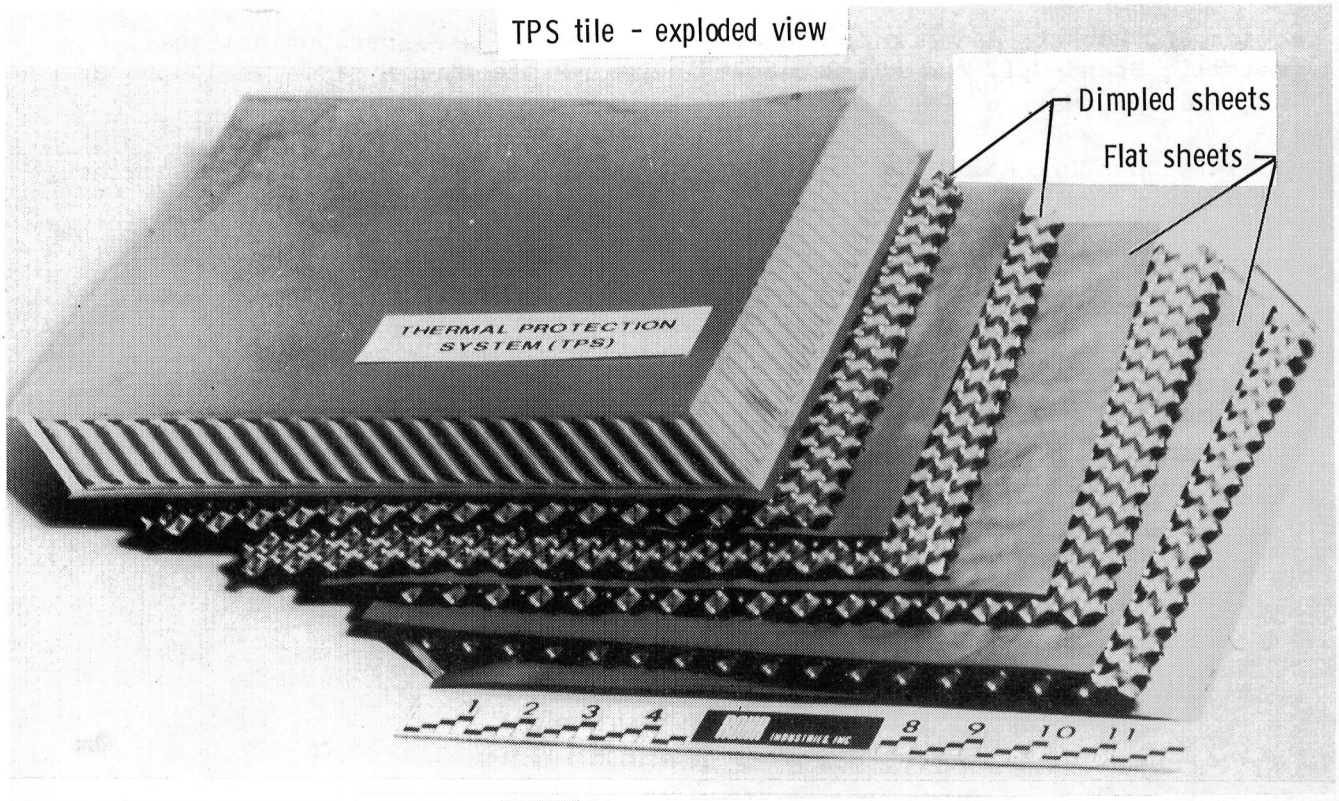

Sandwich cross section

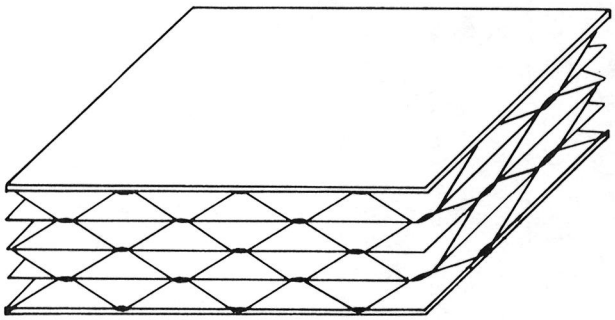

L-83-37

Figure 1.- Titanium multiwall sandwich.

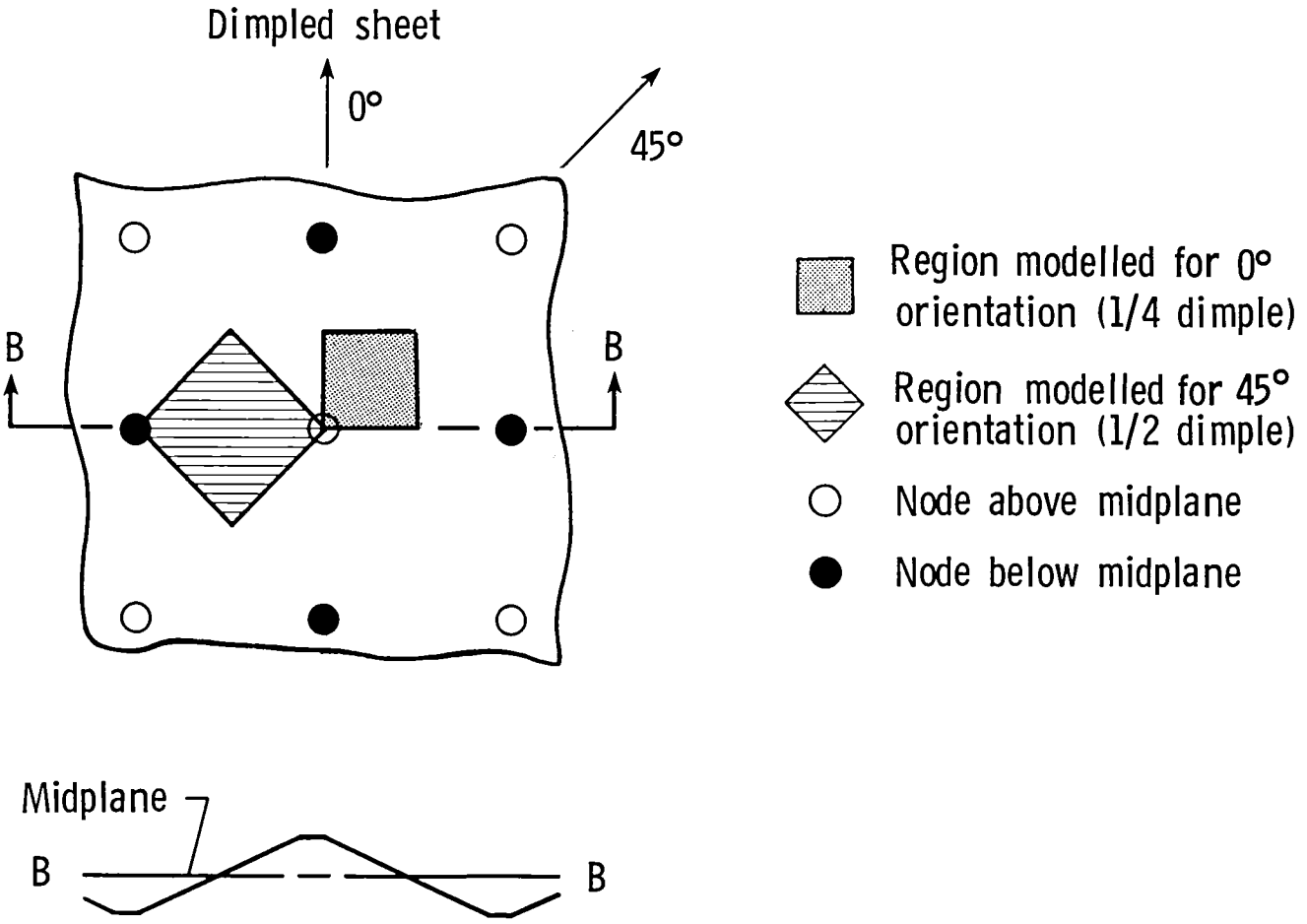

Figure 2.- Regions of dimpled sheet modelled for structural analysis.

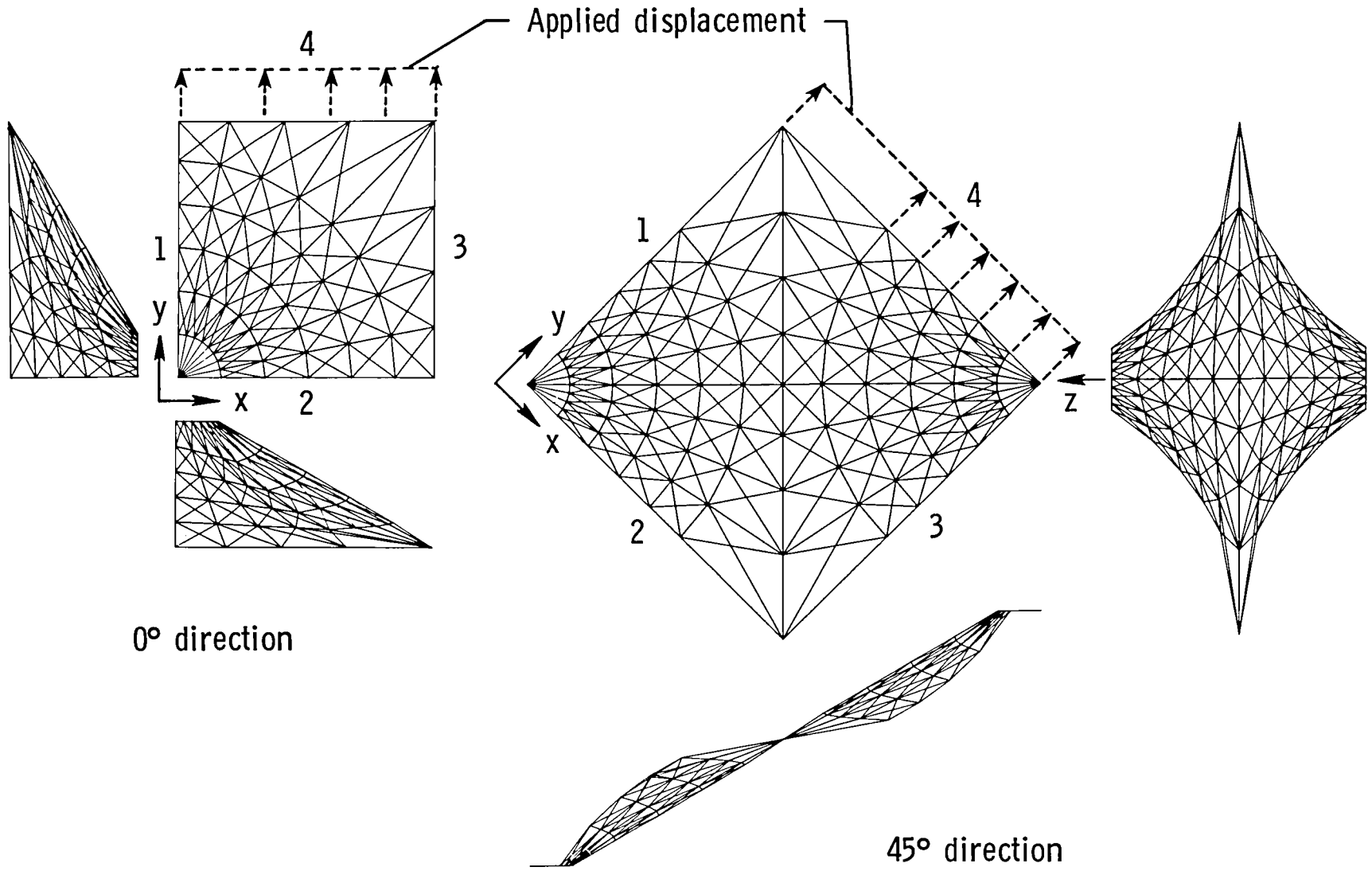

Figure 3.- SPAR finite element models of dimpled sheet.

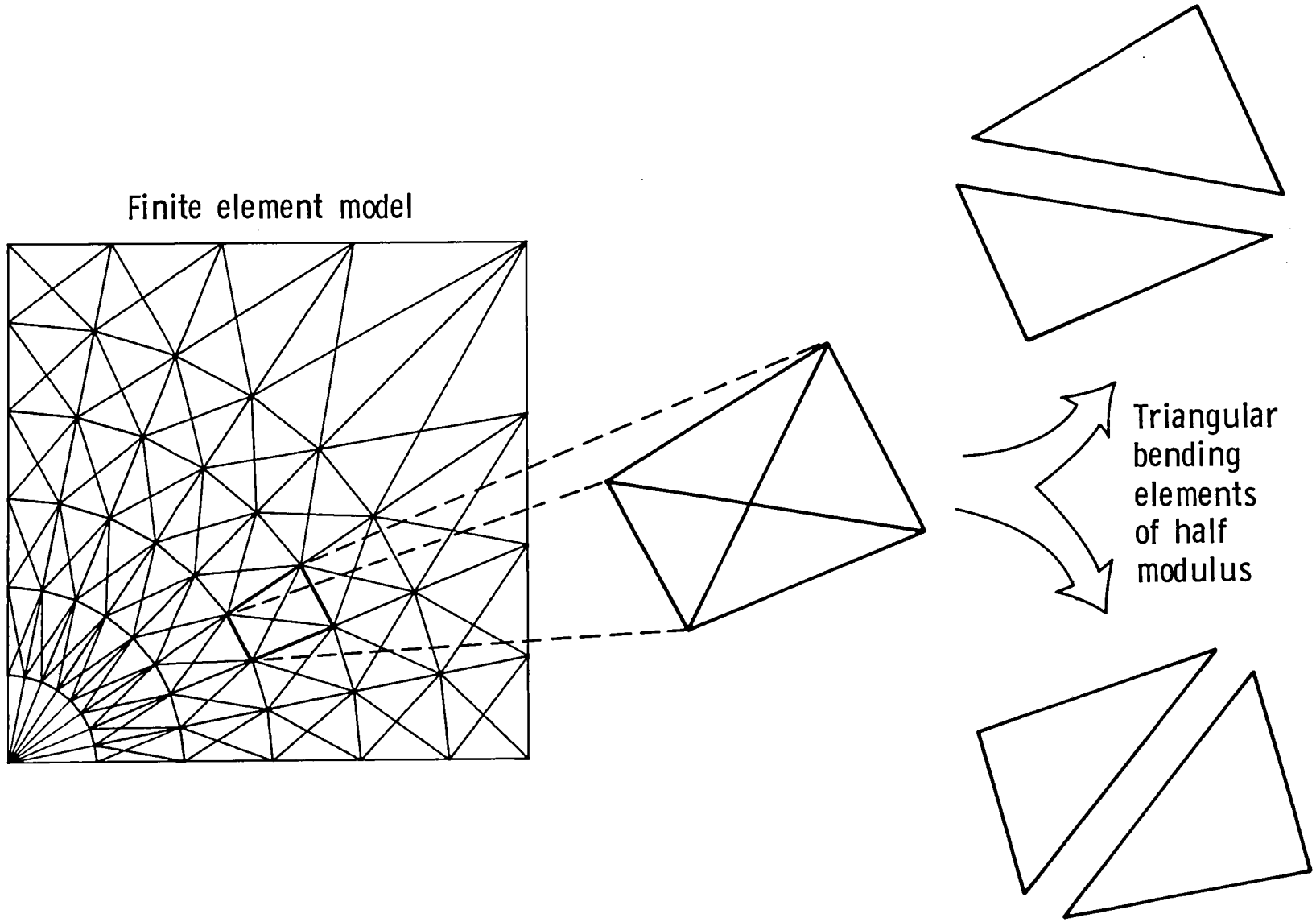

Figure 4.- Illustration of superimposed triangular elements.

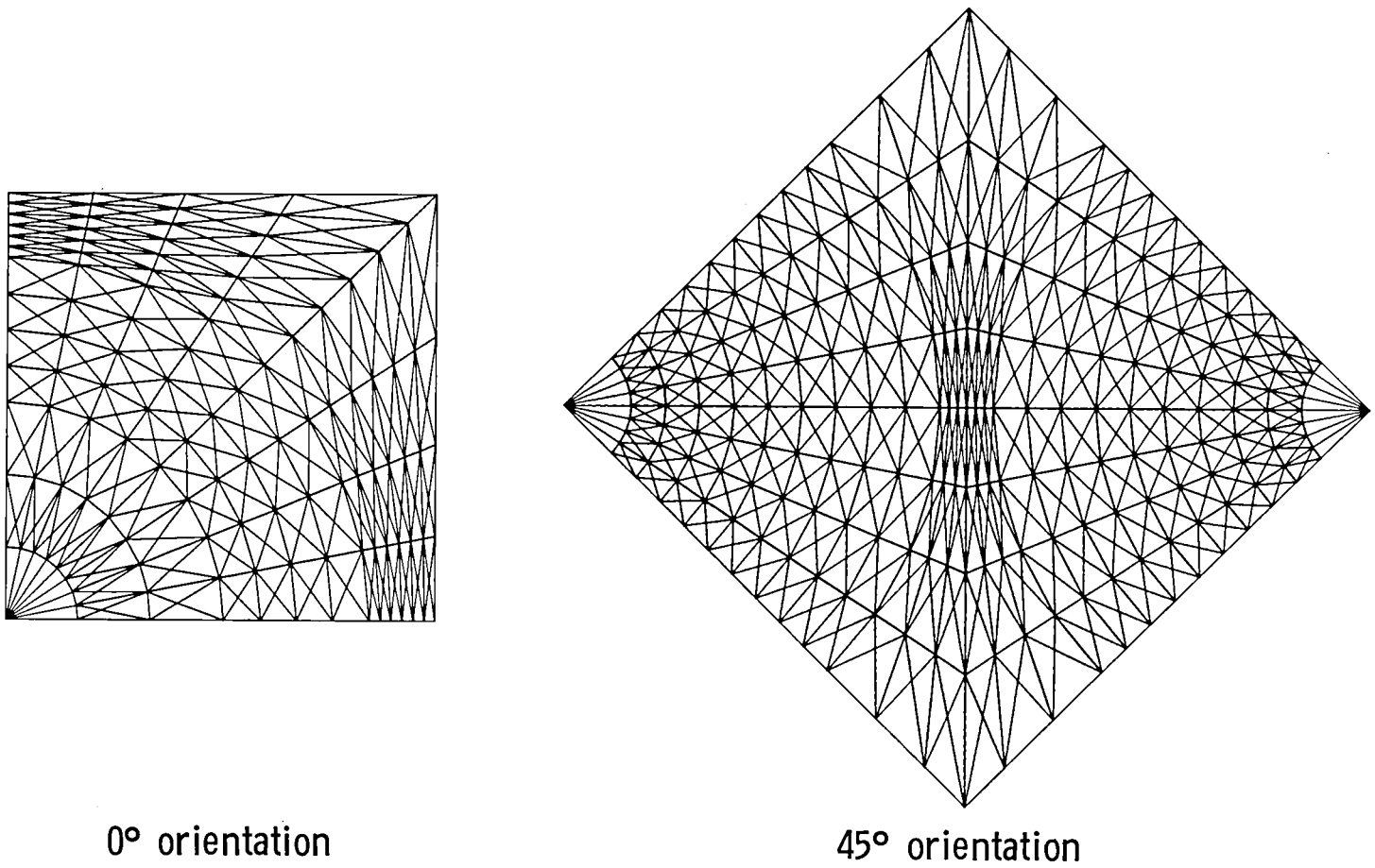

Figure 5.- Finite element models used to calculate stress concentration factors.

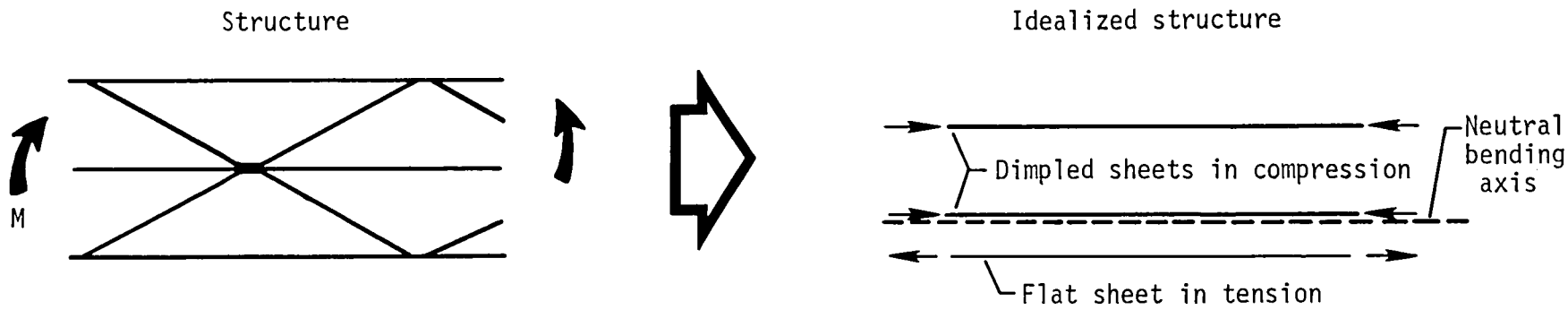

Figure 6.- Illustration of simplifying assumptions used to calculate bending stiffness of multiwall sandwich.

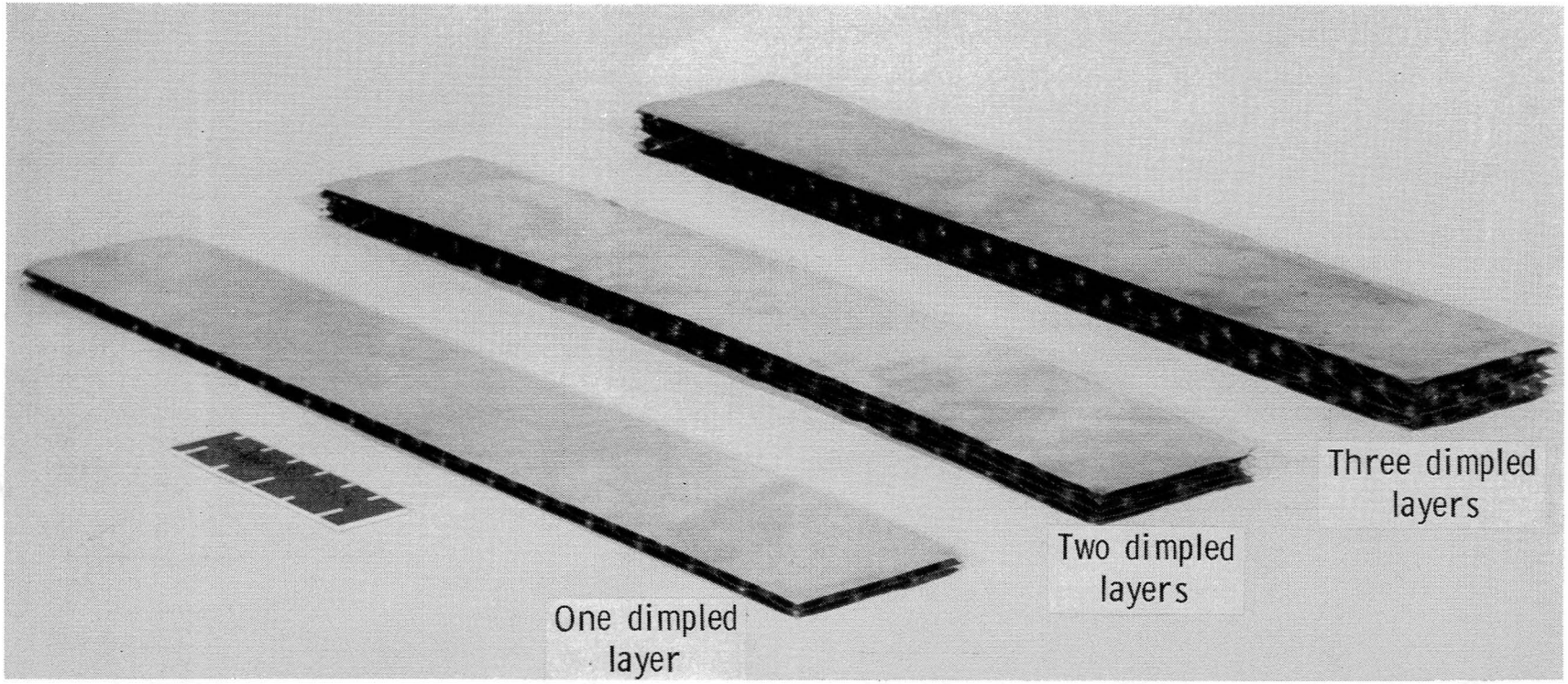

L-82-3152.1

Figure 7.- Bending test specimens.

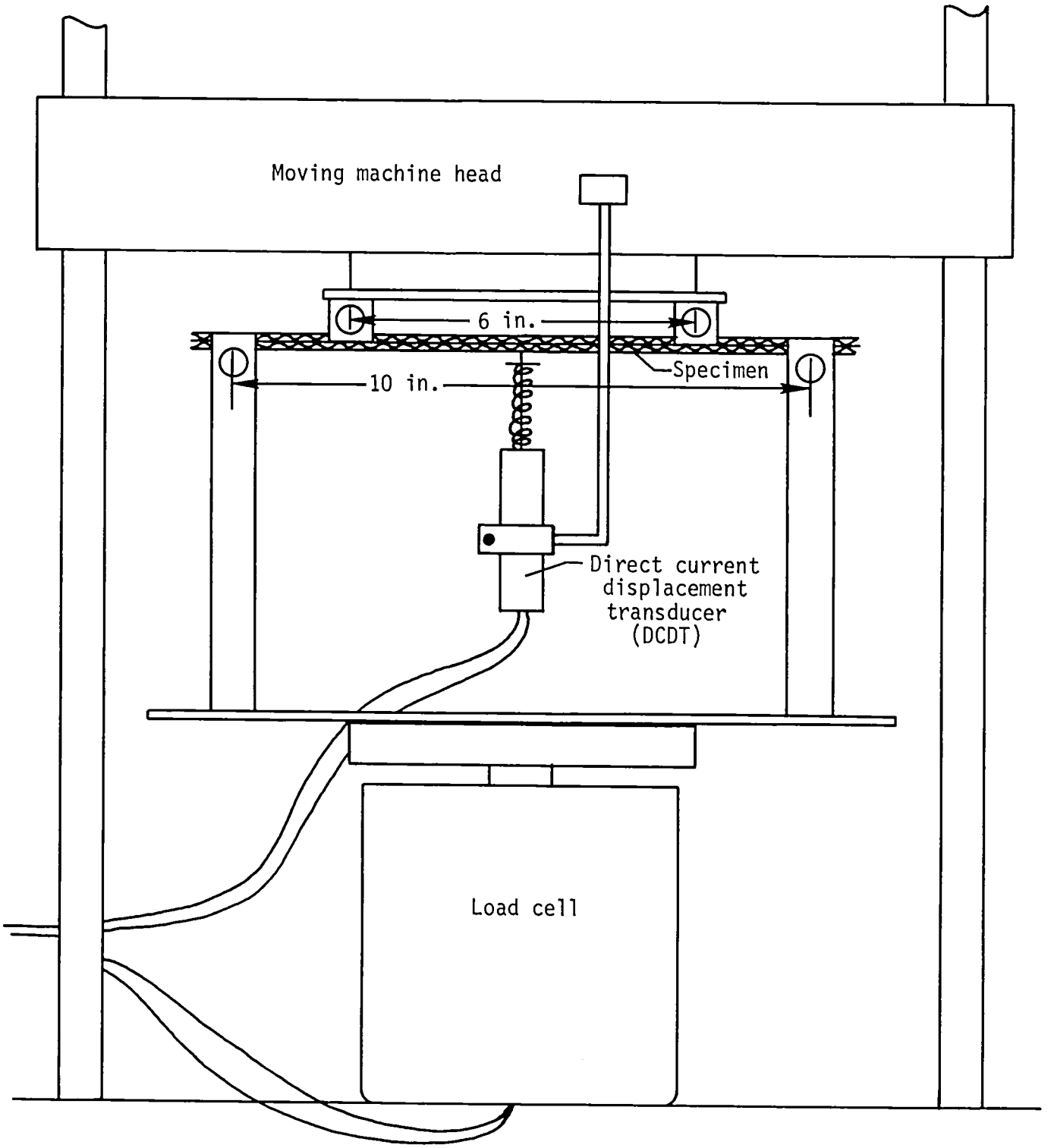

Figure 8.- Four-point bending test setup.

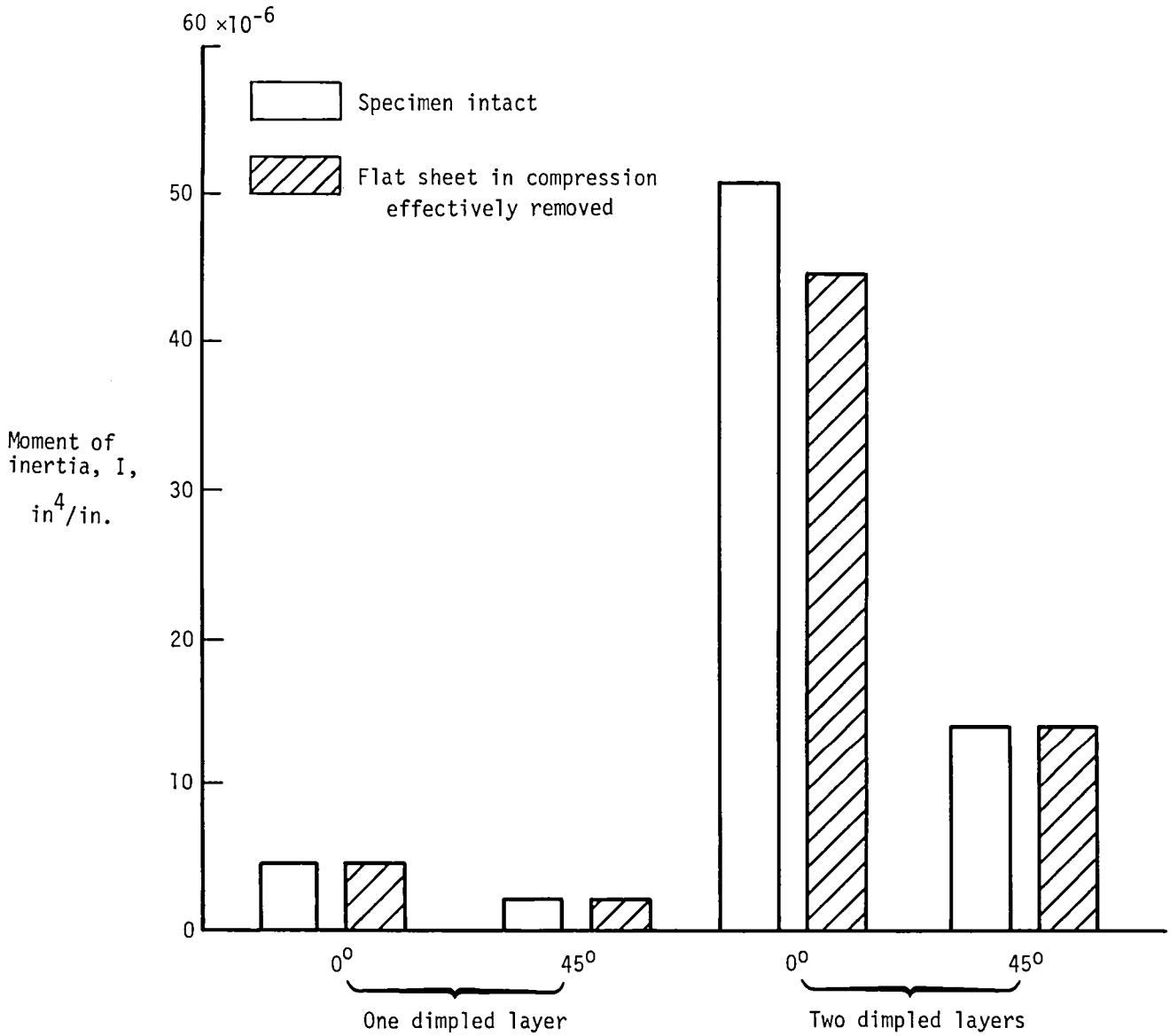

Figure 9.- Effect of flat sheets in compression on moment of inertia of multiwall sandwich. t_f = 0.002 in.

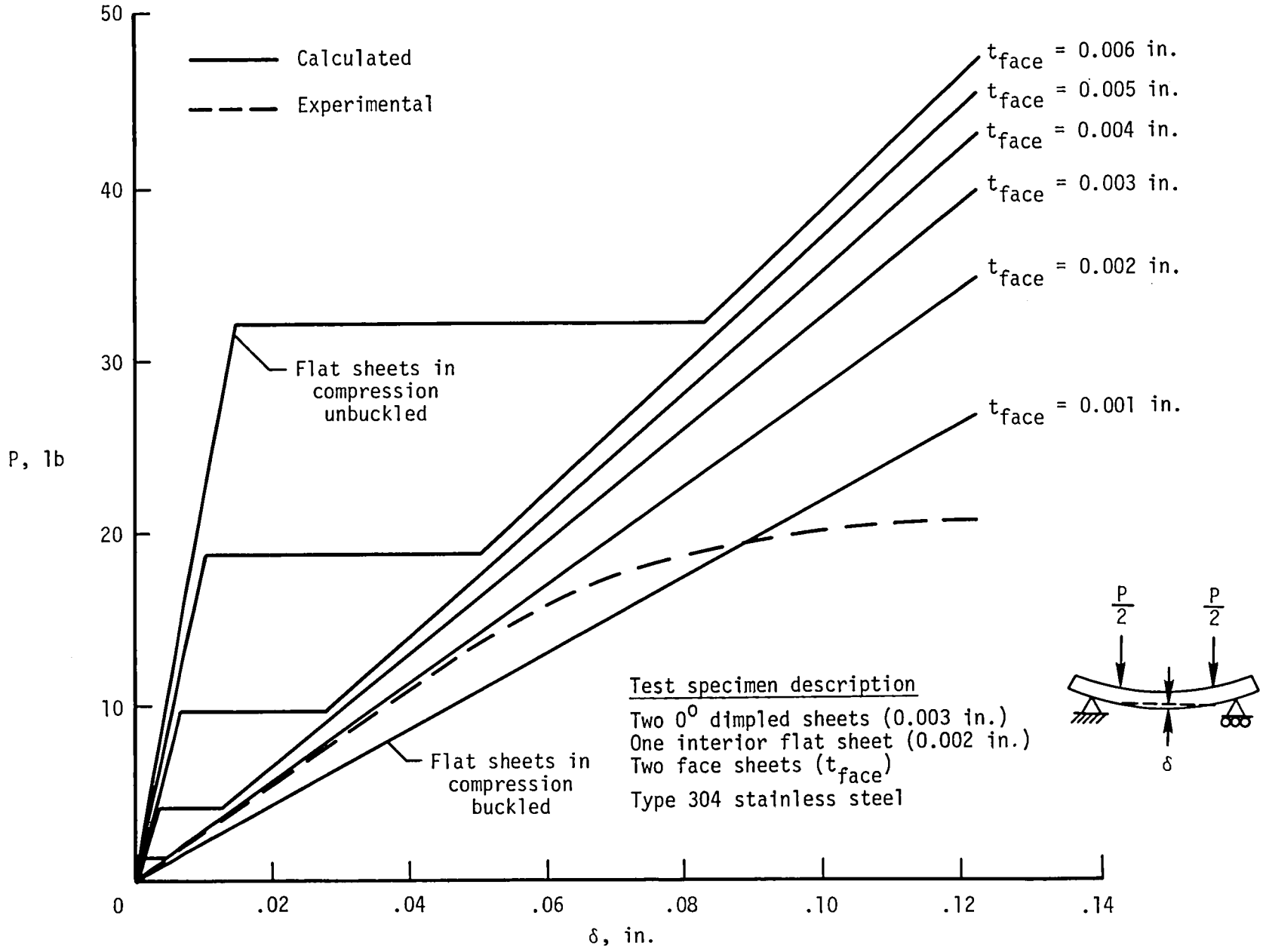

Figure 10.- Predicted load-deflection curves for four-point bending tests on multiwall sandwich.

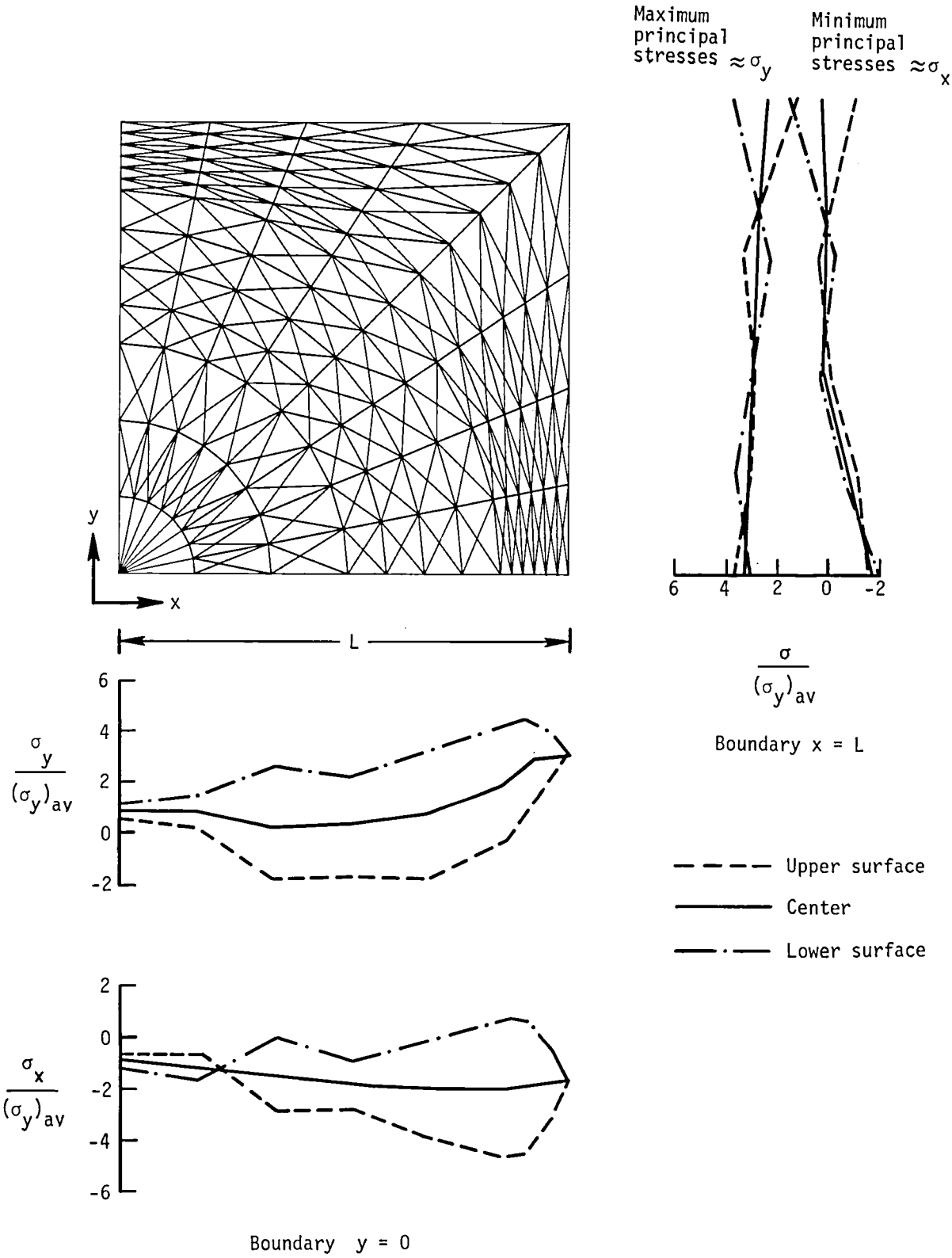

(a) 0° direction.

Figure 11.- Stress concentration factors in dimpled sheet.

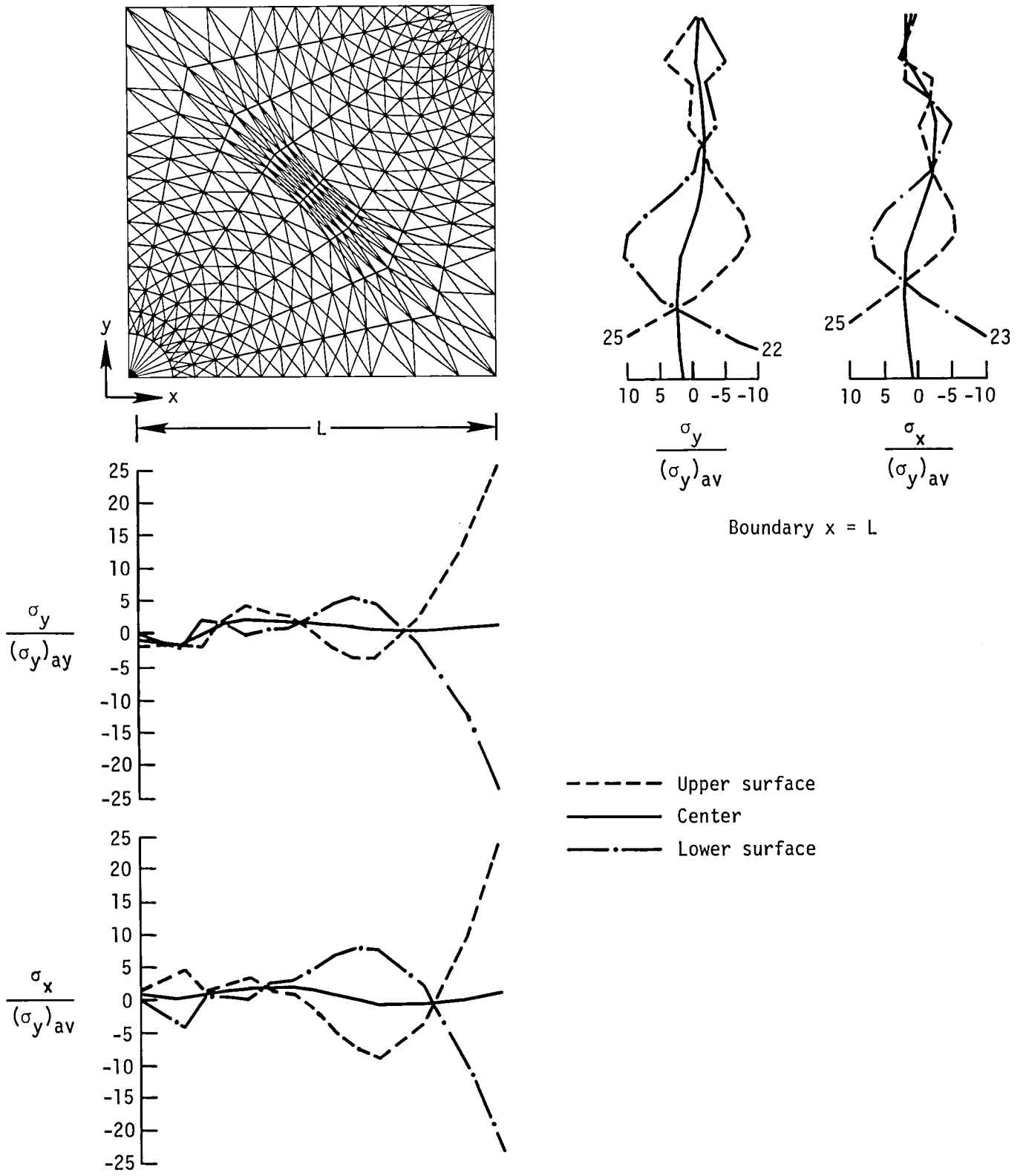

(b) 45° direction; lateral displacement allowed.

Figure 11.- Continued.

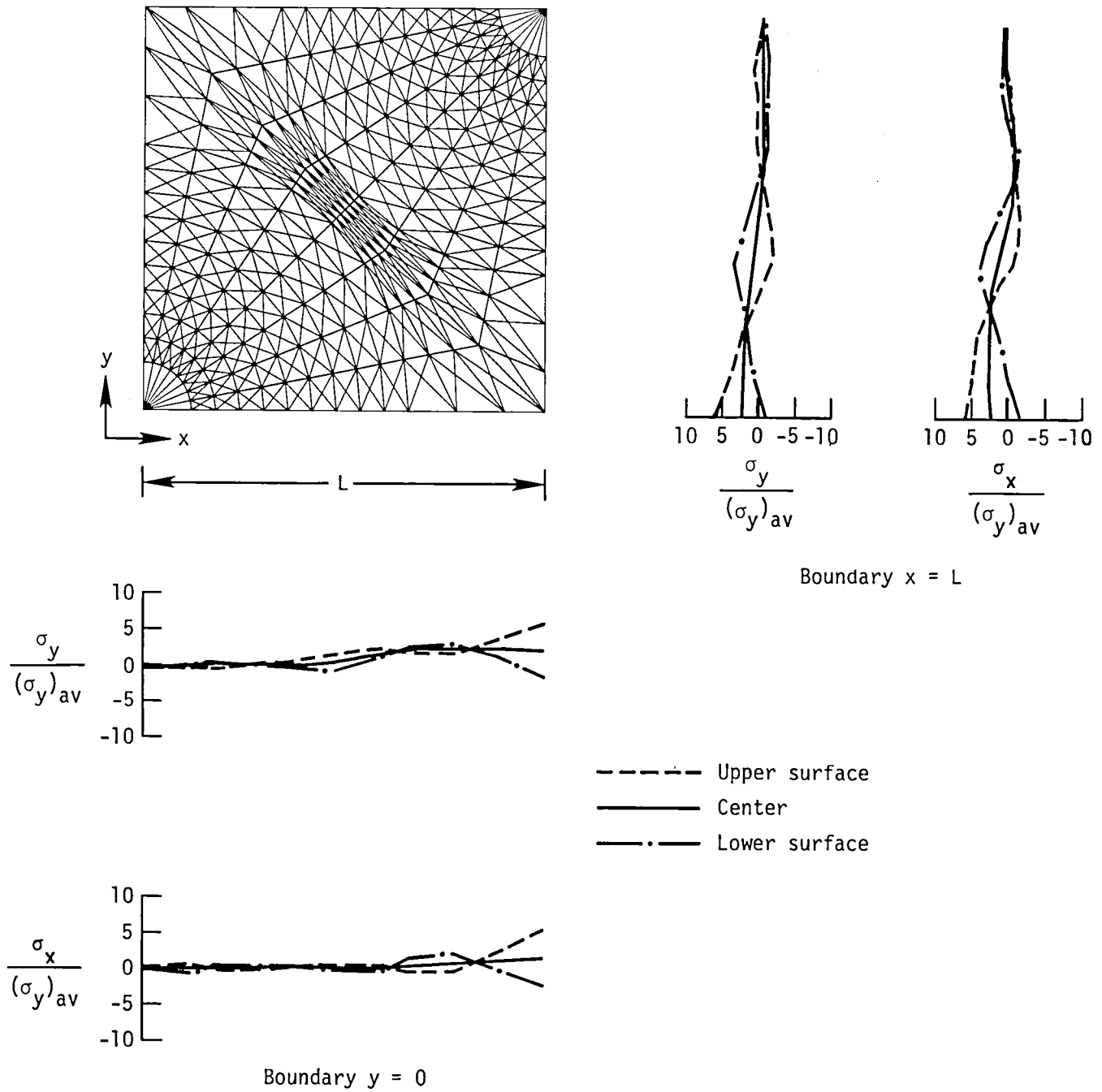

(c) 45° direction; lateral displacement constrained.

Figure 11.- Concluded.

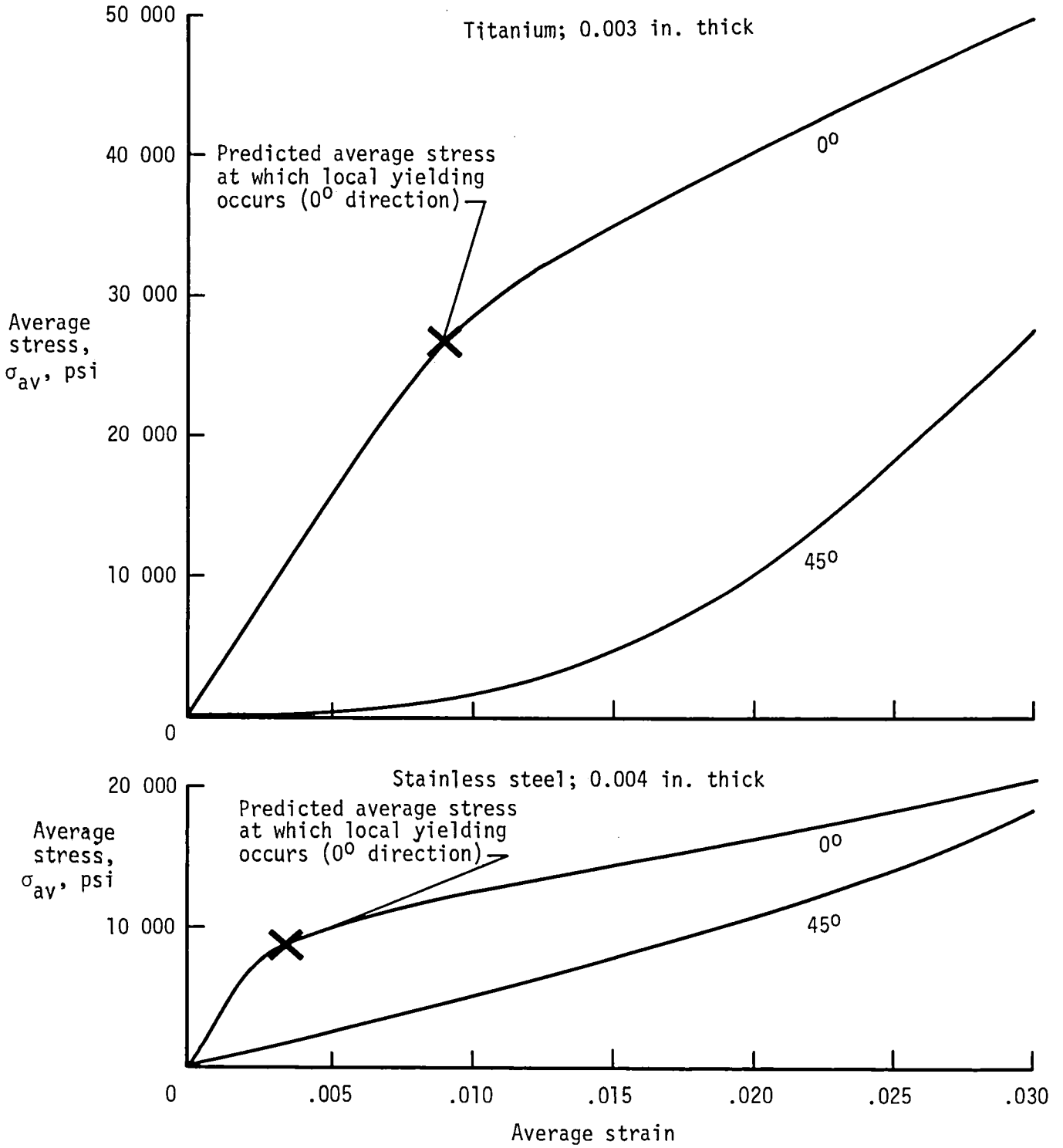

Figure 12.- Stress-strain curves of dimpled sheets (determined from machine-head motion).

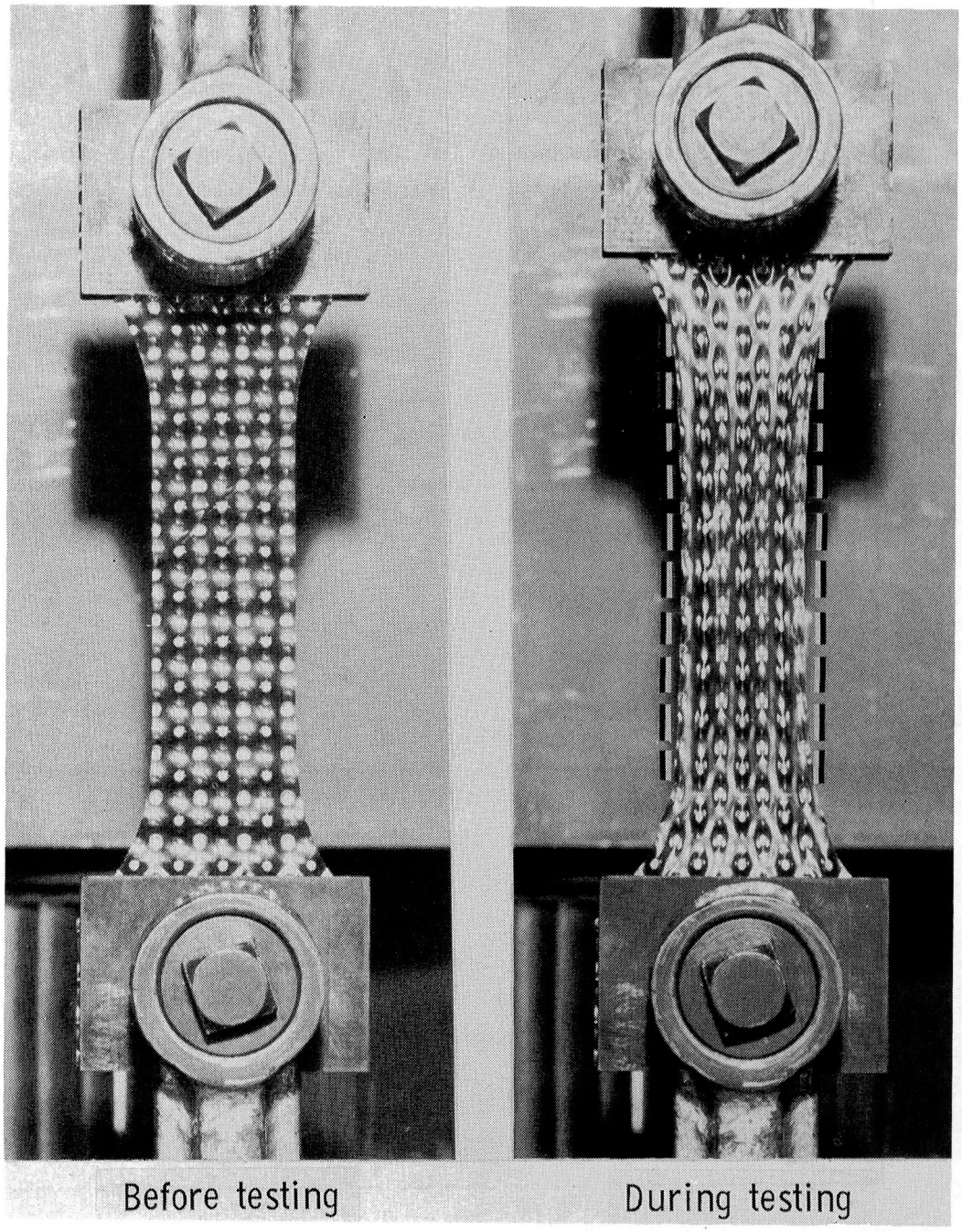

L-83-38

Figure 13.- Observed deformation of dimpled sheet; 45° orientation.

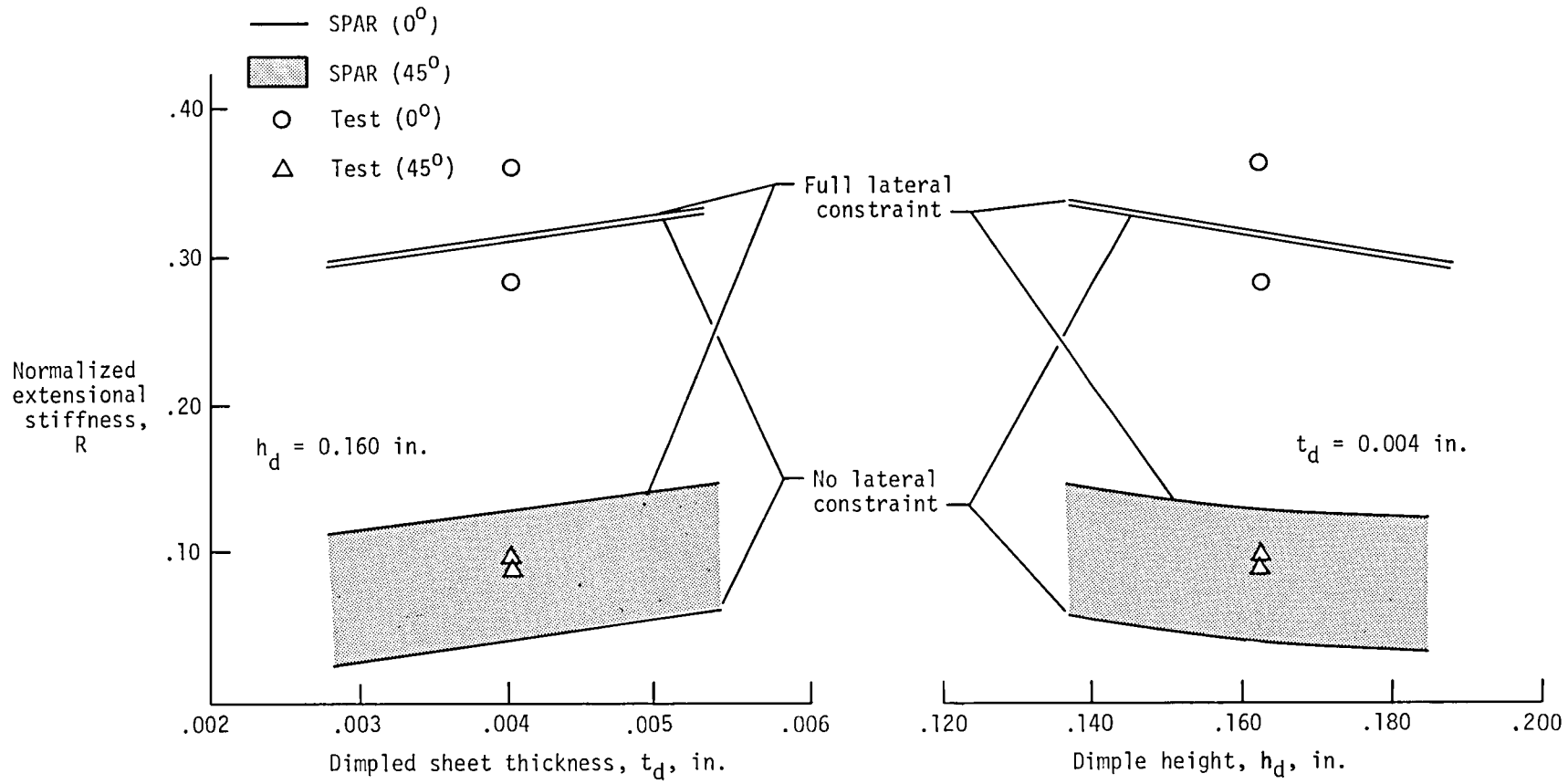

Figure 14.- Normalized extensional stiffness of dimpled sheet.

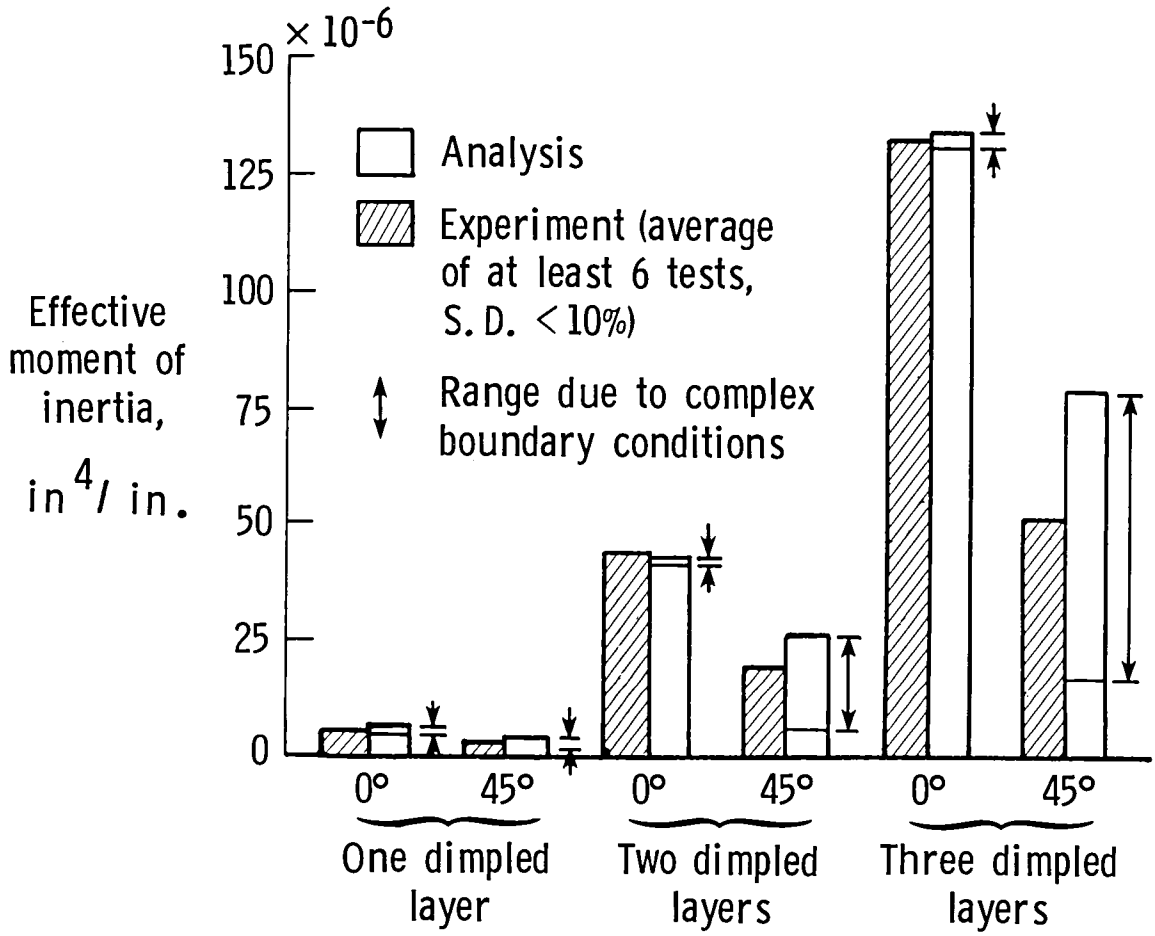

Figure 15.- Effective bending moments of inertia.

1. Report No.	2. Government Accession No.	3. Recipient's Catalog No.
NASA TM-84613		

4. Title and Subtitle	5. Report Date
BENDING STIFFNESS OF MULTIWALL SANDWICH	April 1983
	6. Performing Organization Code 506-53-33-04-00
7. Author(s)	8. Performing Organization Report No.
Max L. Blosser	L-15549
	10. Work Unit No.
9. Performing Organization Name and Address	
NASA Langley Research Center Hampton, VA 23665	11. Contract or Grant No.
	13. Type of Report and Period Covered
12. Sponsoring Agency Name and Address	Technical Memorandum
National Aeronautics and Space Administration Washington, DC 20546	14. Sponsoring Agency Code

15. Supplementary Notes

16. Abstract

An analytical and experimental study was carried out to understand the extensional and flexural behavior of multiwall sandwich, a metallic insulation composed of alternate layers of flat and dimpled foil. The multiwall sandwich was structurally analyzed by using several simplifying assumptions combined with a finite element analysis. The simplifying assumptions made in this analysis were evaluated by bending and tensile tests. Test results validate the assumption that flat sheets in compression do not significantly contribute to the flexural stiffness of multiwall sandwich for the multiwall geometry tested. However, calculations show that thicker flat sheets may contribute significantly to bending stiffness and cannot be ignored. Results of this analytical approach compare well with test data; both show that the extensional stiffness of the dimpled sheet in the 0° direction is about 30 percent of that for a flat sheet, and that in the 45° direction, it is about 10 percent. The analytical and experimental multiwall bending stiffnesses showed good agreement for the particular geometry tested.

17. Key Words (Suggested by Author(s))	18. Distribution Statement
Multiwall sandwich Metallic TPS Bending stiffness	Unclassified - Unlimited Subject Category 39

19. Security Classif. (of this report)	20. Security Classif. (of this page)	21. No. of Pages	22. Price
Unclassified	Unclassified	43	A03

For sale by the National Technical Information Service, Springfield, Virginia 22161

NASA-Langley, 1983

National Aeronautics and
Space Administration

Washington, D.C.
20546

Official Business
Penalty for Private Use, $300

THIRD-CLASS BULK RATE

Postage and Fees Paid
National Aeronautics and
Space Administration
NASA-451

NASA

POSTMASTER: If Undeliverable (Section 158 Postal Manual) Do Not Return